Control of Foxp3$^+$ regulatory T cell abundance and function by distinct signals in different immune environments

Kate Sophie Smigiel

A dissertation submitted in partial fulfillment
of the requirements for the degree of

Doctor of Philosophy

University of Washington
2013

Reading Committee:
Dr. Daniel J. Campbell, Chair
Dr. Pamela J. Fink
Dr. Marion Pepper

Program Authorized to Offer Degree:
Department of Immunology

University of Washington

Abstract

Control of Foxp3^{+} regulatory T cell abundance and function by distinct signals in different immune environments

Kate Sophie Smigiel

Chair of the Supervisory Committee:
Affiliate Professor Dr. Daniel J. Campbell
Department of Immunology

Immune tolerance and activation depend on precise control over the number and function of immunosuppressive Foxp3^{+} regulatory T (Treg) cells. The importance of interleukin (IL)-2 in immune tolerance is demonstrated by the lethal autoimmunity that develops in animals deficient for IL-2 or its receptor; however, IL-2 is not required for Treg cell development, *in vitro* activity, or to maintain total Treg cell numbers. Thus, the precise mechanism by which IL-2 controls Treg cell homeostasis and immune tolerance remains unclear. Here we show that that IL-2 selectively maintains a population of quiescent CD44^{lo}CD62L^{hi} Treg cells that gain access to paracrine IL-2 produced in the T cell zones of secondary lymphoid tissues due to their expression of the chemokine receptor CCR7. By contrast, CD44^{hi}CD62L^{lo}CCR7^{lo} Treg cells that populate non-lymphoid tissues do not respond to IL-2 *in vivo* and are insensitive to IL-2 blockade; instead, their maintenance depends on continued signaling through the co-stimulatory

receptor ICOS. Thus, we define a fundamental homeostatic subdivision in Treg cells based on their localization and provide an integrated framework for understanding how Treg cell abundance and function are controlled by unique signals in different tissue environments.

TABLE OF CONTENTS

LIST OF FIGURES

CHAPTER 1: Introduction

Immune homeostasis

Immune homeostasis ensures that the number, diversity, and functional competency of lymphocytes is maintained, both during periods with and without overt inflammation. The term homeostasis was derived from the Greek word for "stasis", meaning "standing still", although this seemingly restful condition serves to actively replenish the peripheral T cell pool and preserve its functional specialization under steady-state conditions. During inflammation, the outcomes of all immune responses rest on a fulcrum, with homeostasis governing the balance between strong immune responses with potential immunopathology and weak immune responses resulting in unrestrained infection or tumor growth. The homeostatic equilibrium is accomplished through a combination of soluble cytokine signals and cellular interactions between different cell types, which largely occur in a tissue- and microenvironment-specific fashion. Moreover, different populations of cells are placed under unique homeostatic constraints, such that competition for limited resources is minimized via compartmentalization. The study of homeostasis is therefore clinically relevant because proper balance between functional T cell pools contributes to prevent autoimmunity, and this balance can be therapeutically manipulated to prevent conditions such as graft rejection or promote immune responses directed against tumors.

Immune modulation by regulatory T cells

Similar to conventional CD4+ T cells, $CD4^+$ regulatory T (Treg) cells expressing the transcription factor Foxp3 are produced in the thymus but display a distinct T cell receptor (TCR) repertoire that is skewed towards the high-affinity recognition of self-

peptides (Hsieh *et al.*, 2004). Under steady-state conditions, the majority (~80%) of Foxp3+ Treg cells are derived from the thymus (tTreg cell) and express the receptor Neuropilin-1 or the transcription factor Helios; however, Foxp3 can also be induced in conventional CD4+ T cells as a consequence of antigen exposure and the appropriate cytokine environment (e.g., TGF-β), and these induced Treg cells are referred to as peripherally derived (pTreg) cells (Yadav *et al.*, 2013). Functionally, Treg cells are potent anti-inflammatory cells that dampen immune responses to both self and foreign antigens, and these cells have been shown to suppress conventional T cells through multiple mechanisms, including the generation of immunosuppressive cytokines such as tissue growth factor-β (TGF-β) or interleukin (IL)-10 and via direct contact with effector T cells or antigen-presenting cells (APCs) (Takahashi *et al.*, 1998; Read *et al.*, 2000). Indeed, Treg cells are critical for maintaining immune tolerance and preventing autoimmune disease, as evidenced by the widespread autoimmunity that develops in Foxp3-deficient IPEX (immunodysregulation polyendocrinopathy enteropathy X-linked syndrome) patients and scurfy mice (Sakaguchi *et al.*, 2003; Sakaguchi *et al.*, 2008).

Many parallels have been drawn between Treg cells and conventional CD4+ T cells in terms of their ability to co-opt similar transcriptional and activation profiles to respond to specific types of inflammation (Koch *et al.*, 2009; Chaudhry *et al.*, 2009; Zheng *et al.*, 2009). However, despite the considerable body of literature showing how unique subsets of memory CD4 cells rely on distinct homeostatic factors (such as different combinations of the gamma-common (γ_c) chain cytokines IL-2, IL-7, and IL-15), the homeostatic mechanisms that maintain Treg cell complexity remain poorly understood. Thus, the current work sought to identify the cytokine-, cell type-, and tissue-specific factors governing Treg homeostasis *in vivo*.

The role of IL-2 in peripheral Treg homeostasis

IL-2 was originally characterized as a potent T cell growth factor, promoting the expansion of antigen-activated T cells in an autocrine manner. This cytokine is produced mainly by activated CD4+ and CD8+ T cells in secondary lymphoid tissues, where it is consumed primarily by cells expressing the high-affinity form of the IL-2 receptor (Malek, 2008). High-affinity signaling is made possible by the association of CD25 (also known as IL-2Rα) with dimers of CD122 (IL-2Rβ) and CD132 (the γ_c chain), and signal transduction occurs via activation of the Janus kinase (Jak)/signal transducer and activator of transcription (Stat) pathway (primarily via dimers of phosphorylated Stat5), as well as mitogen-activated protein kinase (MAPK) and phosphoinositide 3-kinase (PI3K) signaling. Other γ_c chain cytokines such as IL-7 and IL-15 are also capable of transducing Stat5 signals, and these cytokines have been shown to play important roles throughout T cell development. Although Treg cell thymic development requires T cell-intrinsic Stat5 signaling, this function is mediated primarily by IL-2, with minimal roles for IL-7 and IL-15 that only partially compensate for the loss of IL-2 (Vang *et al.*, 2008; Burchill *et al.*, 2007). The role of IL-2 in the thymic generation of Treg cells has been expertly reviewed elsewhere (Cheng *et al.*, 2011; Mahmud *et al.*, 2013).

Rather than directly participating in IL-2 signaling, CD25 instead serves to increase the affinity of the IL-2R for its ligand by 10- to 100-fold. The main consequences of IL-2 signaling include cell cycle progression and the expression of anti-apoptotic proteins such as Bcl-2 (Deng *et al.*, 1993). In addition, IL-2 signaling upregulates CD25 expression, thereby generating a positive feedback loop (Kim *et al.*, 2001). Many immune cell types, including CD4+ T cells, CD8+ T cells and NK cells, can upregulate CD25 expression upon activation, but Treg cells express constitutively high levels of the high-affinity IL-2 receptor, which is likely due to their high degree of self-reactivity and continuous IL-2 signaling. However, because Runx1 cooperates with Foxp3 and NFAT to bind to the IL-2 promoter and halt its

transcription, Treg cells do not themselves produce IL-2 and are instead reliant on paracrine IL-2 produced by other activated T cells (Ono *et al.*, Nature 2007). Thus, the influence of IL-2 on Treg cell homeostasis is dependent on both the rate of IL-2 production and the rate of IL-2 consumption in the steady state.

The key finding showing the important role for IL-2 in Treg cell homeostasis came from the surprising discovery of the autoimmune manifestations that occur in mice deficient for IL-2 or CD25. Instead of immunodeficiency, which was expected to result from the loss of an important T cell growth factor, animals lacking IL-2 signaling demonstrate over-active T cell responses, massive lymphoproliferation, lymphadenopathy, and splenomegaly and succumb to disease within 6-8 weeks of life. Because Treg cells were first identified by their high-level expression of CD25, the apparent lack of Treg cells in mice deficient for IL-2 or its receptor led to the conclusion that these autoimmune manifestations were the result of decreased Treg cells and their failure to control autoreactive, inflammatory responses (Malek *et al.*, 2002). However, the subsequent identification of Treg cells based on Foxp3, as well as the development of mice in which *Foxp3* expression could be directly identified using fluorescent proteins such as green fluorescent protein (GFP), revealed that CD25-deficient mice contain near-normal frequencies and numbers of Treg cells in both the thymus and periphery (Fontenot *et al.*, 2005). Also, mice in which the IL-2R β-chain is only expressed in the thymus, resulting in T cell unresponsiveness to IL-2 *in vivo*, fail to demonstrate the lethal autoimmunity observed in IL-2Rβ-deficient animals (Malek *et al.*, 2000). Moreover, in contrast to scurfy mice, which lack all Treg cells due to mutation in *Foxp3*, CD25-deficient mice exhibit less severe autoimmune disease and a lifespan that is approximately twice as long as that of scurfy mice. Thus, the role of IL-2 in controlling Treg cell abundance and activity is more complicated than previously appreciated, and although IL-2 is required to

maintain Treg-mediated tolerance *in vivo*, these findings indicate that the peripheral homeostasis of Treg cells is at least partially IL-2-independent.

The precise role for IL-2 in Treg cell survival versus function remains debated. Indeed, because Treg cell numbers have been directly linked to their ability to control the size of effector T cell populations, there is likely considerable overlap between survival and function. Evidence in support of a role for IL-2 in Treg cell function includes the observation that IL-2 neutralization *in vivo* results in the development of autoimmune gastritis on the Balb/c background and exacerbated diabetes on the NOD background (Setoguchi *et al.*, 2005). In fact, spontaneous autoimmunity in NOD mice is genetically dependent on alterations in the *Il2* gene that result in lower production of IL-2 and consequent autoimmune-mediated diabetes through the impaired regulation of Treg cells. Accordingly, IL-2 therapy using anti-IL-2-IL-2 immune complexes, which increases Treg cell numbers by selectively stimulating $CD25^+$ cells (Boyman *et al.*, 2006), was shown to prevent the development of diabetes (Tang *et al.*, 2008) and the induction of experimental autoimmune encephalomyelitis (EAE) and as well as induce tolerance to major histocompatibility complex-incompatible pancreatic islet transplantation (Webster *et al.*, 2009). In addition, Foxp3 function is closely linked to Treg cell fitness and establishment of the Treg cell transcriptional program, and deficiency in CD25 has been shown to result in lower amounts of Foxp3 (Gavin *et al.*, 2007). In fact, forced expression of Foxp3 in IL-2Rβ-deficient mice restored Treg cell function and prevented autoimmunity, demonstrating that IL-2 signaling is functionally linked to the control of Foxp3 expression (Soper *et al.*, 2007). In contrast, the *in vitro* suppressive function of Treg cells isolated from CD25-deficient mice was shown to be intact, and gene expression analysis suggested that the failure of these cells to control the development of autoimmunity was instead related to impaired metabolic fitness (Fontenot *et al.*, 2005). To address the function of Treg cells independent of

the pro-survival effects of IL-2, Il-2-knockout mice were crossed to Bim-knockout mice. However, the enhanced survival of Treg cells via deletion of this pro-apoptotic factor failed to prevent autoimmune disease development, indicating that despite its ability to induce Treg survival, the principle effect of IL-2 on Treg cell function is qualitative rather than quantitative (Barron *et al*., 2010). In addition, apoptosis has been recently highlighted as a critical component of Treg homeostasis. Due to their high rate of steady-state proliferation and the pro-apoptotic effects of Foxp3 itself (Tai *et al.*, 2013), it is not surprising that Treg cells must coordinate survival and death signals to maintain stable numbers. In fact, a recent study linked IL-2-driven upregulation of the pro-survival Bcl-2 family member Mcl-1 to Treg cell survival and showed that depletion of Mcl-1 (with the corresponding unrestrained action of Bim) caused a rapid loss of Treg cells and the onset of fatal autoimmunity (Pierson *et al.*, 2013). Therefore, IL-2 has pleiotropic effects on Treg cell survival and function, and the specific requirement for IL-2-mediated signals likely differs under different conditions.

The notion that γ_c cytokine requirements fluctuate with the development of distinct cell populations is a theme that has been extensively studied in conventional T cells. Naïve T cells primarily rely on IL-7 signals for survival, and in many ways, the role of IL-7 in naïve T cell homeostasis is analogous to the role of IL-2 in Treg homeostasis. For example, conventional T cells do not produce IL-7 and instead rely on stromal cell production of this cytokine within the T cells zones of secondary lymphoid tissues (Link *et al.*, 2007). Moreover, IL-7 signaling primarily regulates T cell survival by inducing the expression of key anti-apoptotic proteins, such as Bcl-2 and Mcl-1, while inhibiting the expression of pro-apoptotic factors such as Bid, Bim, and Bad (Wojciechowski *et al.*, 2007); at the same time, IL-7 has a minimal effect on naïve T cell proliferation. In contrast, effector and memory T cell subsets rely on combined signals from IL-2 and IL-15. Although early activated T cells produce IL-2,

numerous studies have suggested that the initial cycling of antigen-activated T cells is IL-2 independent; instead, for both CD4+ and CD8+ T cells, IL-2 has been shown to be required for the successful generation of effector responses and the programming (during initial expansion) of memory responses (Dooms *et al.*, 2004; Williams *et al.*, 2006). In addition, a recent report showed that although initial memory Treg cell generation requires IL-2, the continued maintenance of this memory subset in the periphery is IL-2-independent (and instead relies on IL-7) (Gratz *et al.*, 2013). Together, these data indicate that IL-2 should no longer be considered a pan-Treg cell survival factor.

T cell receptor signaling and transcriptional control over Treg homeostasis

The high degree of self-reactivity among Treg cells indicates the potential for frequent encounters with antigen in the periphery. Indeed, Treg cells from transgenic mice expressing GFP from the immediate early gene *Nr4a1* (Nur77) locus demonstrated heightened and sustained TCR signaling in comparison to conventional T cells, independent of co-stimulation (Moran *et al.*, 2011). To evaluate the requirement for continued TCR signaling in Treg cell function and homeostasis, another recent study inactivated $p56^{Lck}$ in Treg cells using *Ox40-cre* and a conditional null allele of the *Lck* gene and observed impaired turnover, loss of suppressive function, and dramatic changes in Treg gene expression (Kim *et al.*, 2009). Immediately downstream of the TCR complex, the tyrosine kinase Zap70 is recruited to phosphorylated immunoreceptor tyrosine-based activation motifs (ITAMs), where it is phosphorylated by Lck and becomes catalytically active. Because Zap70 is critically required for thymic T cell development, its role in peripheral T cell homeostasis was not evaluated until recently. By generating mice expressing a Zap70 mutant whose catalytic activity could be selectively blocked with a small-molecule inhibitor, Au-Yeung *et al.* (2010) showed that whereas the catalytic activity

of Zap70 was required for activation of conventional naïve, effector, and memory T cells, the Zap70 kinase-independent pathway was sufficient for Treg cell *in vitro* suppression. Thus, although conventional T cells and Treg cells possess similar molecular machinery to respond to TCR signals, the orchestration of these signals differs dramatically between cell types.

Despite the increased basal level of TCR signaling in Treg cells, activation of the PI3K-Akt pathway downstream of TCR signals is inhibitory to Treg cell differentiation and expansion. Accordingly, reduced levels of active Akt resulting from a kinase-inactive form of PI3K p110δ or deficiency in sphingosine 1-phosphate receptor 1 (S1P1) were shown to favor Treg cell development (Patton *et al.*, 2006), whereas overexpression of constitutively active Akt or S1P1 led to reduced Treg cell frequencies (Liu G *et al.*, 2009; Haxhinasto S *et al.*, 2008). In response to TCR signaling, certain transcription factors (e.g., AP-1, NFAT, and NF-kB) are activated whereas others are inactivated (e.g., Foxo1) in Treg cells. In contrast to factors such as NFAT or NF-kB that translocate from the cytosol to the nucleus upon TCR simulation, Foxo proteins are excluded from the nucleus in response to TCR-induced Akt activation. Thus, the high levels of nuclear Foxo1 in Treg cells compared to conventional T cells are associated with significantly blunted Akt activation, and Treg cells appear to be resistant to the TCR-induced clearance of Foxo1 from the nucleus compared to conventional T cells (Ouyang *et al.*, 2012). Although Foxo family transcription factors have been long known to control Treg cell lineage commitment, recent work has highlighted the role of Foxo1 in peripheral Treg cell homeostasis, as mice with Treg cell-specific deletion of Foxo1 develop a fatal inflammatory disorder similar to that seen in Foxp3-deficient mice, but without any effect on the total number of Treg cells present (Ouyang *et al.*, 2012). Another example of the negative regulation of Treg cells by Akt is demonstrated by the expansion of Treg cells in response to rapamycin, an mTOR (mammalian target of rapamycin) inhibitor. mTOR

signaling (resulting from the mTORC1 and mTORC2 complexes) integrates diverse immune signals (TCR signaling, costimulation, IL-2R signaling, etc.) with metabolic cues (such as glucose transport) to direct T cell fate decisions; in fact, mTOR is required for the differentiation of effector CD4+ T cells but is generally regarded as a negative regulator of Treg cell differentiation (Delgoffe *et al.*, 2009). However, a recent study evaluating the role of mTOR signaling in Treg cell homeostasis and function demonstrated that mTORC1 signaling has a positive effect on Treg cell function in mice, as disruption of mTORC1 through Treg-specific deletion of raptor leads to a profound loss of Treg cell suppressive activity *in vivo* and the development of fatal inflammation (Zeng *et al.*, 2013).

The role of costimulation in Treg homeostasis

CD28 was the first costimulatory molecule discovered, and the interaction between CD28 and its ligands CD80 (B7-1) and CD86 (B7-2) remains the best-characterized costimulatory pathway and the subject of active clinical research. All T cells require 2 signals for productive activation: 'signal 1' delivered through the TCR and 'signal 2' provided by costimulatory molecules. CD28 not only lowers the required threshold for T cell stimulation but also initiates a distinct signaling program involving the PI3K and Akt pathways as well as cell survival pathways. Treg cells constitutively express CD28, and removal of CD28 costimulation results in decreased numbers of thymic and peripheral Treg cells, as observed in CD28- and CD80/86-deficient mice (Tang *et al.*, 2003). Although initial reports were hindered by potential *trans* effects of loss of CD28-mediated costimulation on cytokine (especially IL-2) production by effector T cells, a recent study generated CD28-conditional knockout mice and reported the cell-intrinsic requirement for CD28 in Treg cell survival and function, as these mice developed severe autoimmunity with increased numbers of activated effector cells (Zhang *et al.*, 2013). In support of a functional role for CD28 in Treg cells, NOD mice

deficient for either CD28 or its ligands were also shown to develop exacerbated autoimmune disease, whereas transfer of wild-type (WT) Treg cells could prevent the development of diabetes in these mice (Salomon *et al.*, 2000).

The potential for redundancy between CD28- and IL-2-mediated homeostatic signals in Treg cells has been proposed, given that CD28 signaling is known to upregulate CD25 expression on Treg cells and drive IL-2 production by activated CD4+ effector cells. Indeed, data from IL-2/CD28 double knockout mice revealed a more significant decline in peripheral Treg cell frequencies compared to single knockouts alone, indicating an additive role for these homeostatic pathways in Treg cell maintenance (Hoyer *et al.*, 2007). As an important source of costimulatory signals, dendritic cells (DCs) are known to support the maintenance of peripheral Treg cells. In fact, DC numbers are tightly linked to Treg numbers via a regulatory loop, whereby increased numbers of DCs leads to increased Treg cell division and accumulation via a mechanism requiring major histocompatibility complex (MHC) class II expression on DCs (Darrasse-Jeze G *et al.*, 2009). In addition, using mixed chimeras generated by reconstitution with bone marrow from DC-deficient mice and CD80$^{/}$CD86 double knockout mice, Bar-On *et al.* (2011) showed that DCs were the primary cell type responsible for providing CD80/86 co-stimulation to Treg cells.

Similar to CD28, inducible costimulator (ICOS) is another member of the immunoglobulin (Ig)-like family of costimulatory receptors that helps control the development and function of nearly all $CD4^+$ T cell subsets. Expression of ICOS is rapidly induced on T cells following activation and is influenced by both TCR and CD28 signaling; however, ICOS is expressed at higher levels in the steady state by Treg cells compared to conventional T cells. DCs and B cells express high levels of ICOS-ligand (ICOSL), and ICOS has also been shown to control regulatory T cell abundance and function *in vivo*. The number of Treg cells in ICOS-deficient mice is severely reduced, and, in contrast to CD28-deficient animals, this seems to be solely

the result of defective peripheral maintenance, as normal thymic Treg populations were reported in ICOS-knockout mice (Burmeister *et al.*, 2008). Moreover, blockade of ICOS was shown to promote the development of diabetes in BDC2.5 TCR-transgenic mice, as a result of dysregulation of $ICOS^+$, IL-10-producing Treg cells (Herman *et al.*, 2004).

Costimulatory signaling can provide both positive and negative forms of regulation. Signal transduction downstream of the TCR is modulated on the basis of phosphorylation of highly conserved amino acid motifs found in a large number of receptors or adaptor proteins; the 2 main types of such motifs include immunoreceptor tyrosine-based activation motifs (ITAMs) and immunoreceptor tyrosine-based inhibition motifs (ITIMs). Classic ITAM-containing molecules include CD3 and CD28, whereas negative regulatory molecules such as cytotoxic T lymphocyte antigen-4 (CTLA-4) programmed death-1 (PD-1) and killer cell lectin-like receptor G1 (KLRG1) contain ITIMs. KLRG1 is expressed at high levels on activated NK cells and $CD8^+$ T cells (Robbins *et al.*, 2003) and has been shown, under specific conditions, to modulate signals delivered through activating ITAM-containing receptors (Robbins *et al.*, 2002; Ito M *et al.*, 2006; Grundemann C *et al.*, 2006). KLRG1 has classically been used as a marker of $CD8^+$ short-lived effector cells (SLECs), which are generated rapidly following infection, express low levels of the IL-7 receptor, and have a low potential to form memory (Joshi *et al.*, 2007). However, the functional significance of this high-level expression remains largely undetermined. The ligand for KLRG1 is E-cadherin (Grundemann *et al.*, 2006), a transmembrane protein involved in cell-cell adhesion that is expressed by epithelial cells and some DC subsets. Although a significant fraction of mouse $Foxp3^+$ Treg cells expresses KLRG1 (Beyersdorf *et al.*, 2007), the role of this ITIM-containing molecule has not been evaluated in this T cell population. Moreover, because identification of mechanisms capable of restraining Treg activity would be clinically

relevant, the current study to evaluate whether KLRG1 expression on Treg cells may function to negatively regulate the responses of activated Treg cells in peripheral tissues, where the levels of E-cadherin are greatest.

How anatomical location dictates Treg homeostasis

Lymphoid tissues are complex structures where numerous cell types with distinct functions and antigen specificities are organized into specific compartments to facilitate communication and the subsequent generation of a uniform immune response. Migration to and within specific compartments of lymphoid tissues is particularly important for the modulation of antigen-specific responses, and integrin and chemokine signals play a key role in this process. Under steady-state conditions, the chemokines CCL19 and CCL21 are constitutively expressed and act as the sole ligands for the chemokine receptor CCR7, which guides the homing of various T cell populations and antigen-presenting DCs to secondary lymphoid tissues (Forster *et al.*, 2008). CCR7 expression coordinates the homing and positioning of naïve T cells, enables the recirculation of central memory T_{CM} cells through lymphoid tissues, and is also required for Treg cell-mediated control of immune responses. Besides showing grossly altered lymphoid tissue architecture, CCR7-deficient mice display multi-organ autoimmunity associated with deficits in the *in vivo* function of Treg cells resulting from improper selection in the thymus as well as impaired migration in the periphery (Worbs *et al.*, 2007). Although Treg cell *in vitro* suppressive capabilities remain intact in CCR7-knockout mice, the suppressive function of CCR7-deficient Treg cells *in vivo* is profoundly lacking, and this implies that proper lymphoid tissue homing *in vivo* supplies Treg cells with the necessary homeostatic requirements.

In addition to lymphoid tissues, Treg cells can be found in virtually all non-lymphoid tissues, including the skin and hair follicles, lung, liver, intestines, adipose tissue, brain and spinal cord, placenta, tumors, and atherosclerotic plaques (Burzyn

et al., 2013). Although their frequency at these sites is increased during periods of inflammation, Treg cells demonstrate a wide array of homing receptor expression patterns and transcriptional profiles during the steady-state that enable their continued migration and persistence in peripheral tissue sites, similar to effector or memory T cells. Moreover, steady-state homing to non-lymphoid tissues is critical for controlling Treg cell homeostasis and function at these sites. Previous work from our group demonstrated that mice whose Treg cells lack the chemokine receptor CCR4 develop spontaneous inflammatory disease specifically in the skin and lungs (Sather *et al.*, 2007). Similarly, mice deficient in the -1,3-fucosyltransferase VII (FuT7) enzyme, which lack functional ligands for the P- and E-selectin adhesion molecules, demonstrate normal Treg cell numbers and function in skin-draining LNs and other peripheral tissues, but the inability of these Treg cells to access the skin itself results in dysregulated cutaneous immune responses and severe inflammation selectively at this site (Dudda *et al.*, 2008). Therefore, specific homeostatic signals received in peripheral tissues, distinct from those available in lymphoid tissues, are required to regulate cutaneous immune responses. Numerous reports have shown that Treg cells present in peripheral tissues adopt an effector-like phenotype associated with activation and immunomodulatory functions (e.g., IL-10 production). Mechanistically, the transcription factors Blimp-1 and IRF-4 were recently shown to be required for effector Treg cell IL-10 production, ICOS expression, and homeostasis in tissues such as the lung and intestines (Cretney *et al.*, 2011). Interestingly, Blimp-1 was shown to be dispensable for the generation of effector Treg cells, which highlights its role in peripheral tissue homeostasis and explains the immunopathology observed in Blimp-1-deficient mice and mice with Treg-cell specific *Il10* deficiency (Kallies *et al.*, 2006; Rubtsov *et al.*, 2008).

The self-reactivity of Treg cells also contributes to their localization in non-lymphoid tissues, presumably to prevent autoimmune responses and collateral

damage to self during periods of strong inflammation. The recent generation of elegant TCR-transgenic mouse models has significantly contributed to our understanding of how TCR specificity dictates Treg migration, homeostasis, and function. Using the scurfy mouse model of Foxp3 deficiency, a recent study from our lab showed that Treg cells from mice engineered to express an autoreactive TCR displayed an activated phenotype with the expression of skin-homing molecules such as CD103 and E/P-selectin ligands (Killebrew *et al.*, 2011). Similarly, by cloning the TCR of tumor-infiltrating Treg cells in a mouse model of prostate tumor development, another recent study revealed that prostate-specific Treg cells were generated in the thymus and accumulated in peripheral tissues on the basis of antigen recognition (Malchow *et al.*, 2013). To address the continued requirement for antigen signaling by Treg cells in peripheral tissues, Rosenblum *et al.* (2011) developed an ovalbumin (OVA)-specific TCR-transgenic model in which skin-specific expression of OVA could be experimentally induced. These results indicated that expression of an antigen in a peripheral tissue could promote the accumulation of antigen-specific Treg cells required for the resolution of tissue-specific autoimmunity. Moreover, these skin-resident OVA-specific Treg cells were termed memory Tregs because they could survive in this nonlymphoid site for extended periods without antigen expression but were 'primed' to control subsequent inflammation upon forced re-expression of antigen. Together, these studies show how, by virtue of the expression of tissue-restricted TCRs, Treg cells are kept 'poised' under steady-state conditions in peripheral tissues.

CHAPTER 2: Materials and Methods

Mice

C57BL/6 (B6), CD45.1^{+} B6 congenic, B6.*Ccr7*$^{-/-}$, Balb/c, and D011.10 mice were purchased from The Jackson Laboratory. B6.Foxp3^{gfp} mice have been previously described (Fontenot et al., 2005b). B6.*Il2ra*$^{-/-}$ mice were obtained from Jackson Labs and crossed to B6.Foxp3^{gfp} mice. Balb/c mice expressing RIP-mOVA and sOVA were provided by A. Abbas (University of California, San Francisco). Spleens from B6.Nur77^{gfp} mice were kindly provided by K. Hogquist (University of Minnesota). Spleens and thymi from B6.Rag2^{gfp} mice were kindly provided by P. Fink (University of Washington). *Klrg1-/-* mice were kindly provided by Dr. Hans-Peter Pircher (University of Freiburg, Germany). All mice were bred and maintained at either the Benaroya Research Institute or the University of Georgia. All experiments were approved by the Office of Animal Care and Use of the University of Georgia and the Institutional Animal Care and Use Committee of the Benaroya Research Institute.

Flow cytometry and cell sorting

Cells were isolated from various tissues as previously described (Sather *et al.*, 2007). Cell surface staining was performed with the following directly conjugated anti-murine antibodies (from Biolegend unless otherwise specified): anti-CD4 (RM4-5), -CD44 (IM7), -CD62L (MEL-14), -CXCR3 (CXCR3-173), -ICOS (15F9), -CD69 (H1.2F3; BD Biosciences), -CD25 (PC61), -CD45.1 (A20), -CD45.2 (104), -CD103 (2E7; eBiosciences), -KLRG1 (2F1; eBiosciences), and -DO11.10 TCR (KJ-126; eBioscience). To assess CCR7 expression, freshly isolated cells were placed for 1 h at 37°C in complete medium, followed by incubations with CCL19-human IgGFc fusion protein, biotinylated goat-anti-human IgGFc (Jackson Immunoresearch), and

streptavidin-PE-Cy7 (eBioscience) at 4°C. P-selectin ligand expression was evaluated by incubation with P-selectin-IgM fusion protein, followed by biotinylated goat-anti-human IgM (Jackson Immunoresearch) and streptavidin-PE-Cy7. For intracellular staining, cells were surface stained and then permeabilized with eBioscience FixPerm buffer. Cells were then washed and stained with antibodies against Foxp3 (FJK-16s; eBioscience), Ki67 (B56; BD Biosciences), Bcl-2 (BD Biosciences), and/or Helios (22F6, Biolegend). To assess pStat5 levels directly *ex vivo*, spleens were immediately disrupted using glass slides into BD Cytofix/Cytoperm buffer. After incubation for 30 min at room temperature, the cells were washed, resuspended in 400 µl 90% methanol, and incubated on ice for 30 min. After an additional wash, cells were stained for surface and intracellular antigens, including pStat5 (pY694; BD Biosciences), for 45 min at room temperature in the dark. To assess apoptosis after *in vitro* culture, cells were surface stained as described above, washed, and stained with AnnexinV (eBioscience) in 1X Annexin Binding Buffer (eBioscience) for 15 minutes at RT. Cells were then washed, stained with propidium iodide staining solution (eBioscience) and immediately analyzed by FACS. Data were acquired on a LSR II (BD Biosciences) and analyzed using FlowJo software (Treestar). For cell sorting experiments, $CD4^+$ cells were enriched using CD4 Dynabeads (Invitrogen), stained for desired cell surface markers, and sorted using a FACS Vantage or Aria (BD Biosciences).

In vivo **T cell labeling**

Two micrograms of anti-CD4 PE (RM4-4; Biolegend) was injected intravenously (i.v.), and mice were sacrificed 5 min after injection. Splenocytes were prepared for flow cytometry analysis as described above, with CD4 surface staining using RM4-5 antibodies.

Adoptive transfer experiments

Two hundred thousand FACS-sorted WT $CD4^+Foxp3^+CD44^{lo}CD62L^{hi}$ cT_R cells and $CD4^+Foxp3^+CD44^{hi}CD62L^{lo}$ eT_R cells were labeled with eFluor670 cell proliferation dye (Ebioscience) and transferred i.v. into congenically mismatched recipients. Transferred cells were recovered after 7 or 15 days and analyzed by flow cytometry; in the 7-day experiment, recipient animals received anti-IL-2 injections on days 0, 3, and 6. FACs-sorted $CD4^+Foxp3^{gfp+}$ T cells from $CD45.1^+$ B6.SJL and $CD45.2^+$ *Il2ra*$^{-/-}$ mice were co-transferred into $CD45.2^+Foxp3^{gfp-}$ recipients, and transferred cells were recovered from the spleen 7 d after transfer and analyzed by flow cytometry. Two hundred thousand FACS-sorted $CD4^+Foxp3^+CD44^{lo}CD62L^{hi}$ Treg cells from $CD45.1^+$ WT or $CD45.2^+$ *Ccr7*$^{-/-}$ mice were i.v. transferred to congenically marked recipient mice. In similar experiments, $CD4^+$ cells were purified from WT spleens using CD4 Dynabeads (Invitrogen), and then $CD25^+$ cells were enriched using CD25-PE and anti-PE Microbeads (Miltenyi Biotech). Enriched $CD4^+CD25^+$ cells were then cultured in complete medium alone or with pertussis toxin (ptx) (List Biological Laboratories) at 100 ng/mL for 2 h *in vitro* and transferred to congenically marked recipient mice. Splenocytes of recipient mice were harvested 36 h after transfer and analyzed by flow cytometry. Enriched $CD4^+CD25^+$ cells from DORmO spleens were labeled with CFSE, and $1x10^6$ cells were transferred i.v. to recipient animals. In some experiments, mice received 25 µg LPS i.v. at the time of cell transfer. Transferred cells were recovered 6 d after transfer and analyzed by flow cytometry.

Quantitative PCR

RNA extraction was performed using Qiagen RNeasy columns (Qiagen), and cDNA was generated using Omniscript RT Kit (Qiagen) according to the manufacturer's instructions. Presynthesized Taqman Gene Expression Assays (Applied Biosystems) were used to amplify *Mcl1* (Mm00725832_s1) or *Ccr7* (Mm01301785_m1) mRNA

transcripts. *Actb* was used as an internal control, and target gene values are expressed relative to *Actb*.

Immunofluorescence microscopy

Five-micron thick frozen sections of OCT-embedded spleens, peripheral lymph nodes, small intestines or Peyer's patches were fixed with 3.2% formaldehyde (Polysciences, Inc.), permeabilized in 90% methanol, and stained with anti-CD5 (53-7.3; Biolegend) conjugated to AlexaFluor488, biotinylated anti-Foxp3 (FJK-16s; eBioscience) visualized with AlexaFluor647-conjugated streptavidin, anti-pStat5 (pY694; D47E7; Cell Signaling) visualized with AlexaFluor555-conjugated anti-rabbit IgG $F(ab')_2$ (Cell Signaling), or biotinylated anti-MAdCAM-1 (MECA-367; eBioscience) visualized with AlexaFluor555-conjugated streptavidin. Images were acquired on a Leica TCS-SP5 II confocal microscope and analyzed using NIH Image J software.

Antibody treatment

Mice were given 150 µg of the indicated antibodies (JES6-1A12, anti-IL-2; S4B6-1, anti-IL-2; HK5.3 anti-ICOSL, all from BioXCell) or an equivalent amount of rat IgG (Sigma) by intraperitoneal injection on days 0, 3, and 6 and sacrificed for analysis on day 7 or on days 0, 3, 6, 9, and 12 and sacrificed on day 14.

B16.Flt3L tumors

Recipient mice were given $3x10^6$ control or Flt3L-secreting B16 cells by subcutaneous injection, and were sacrificed ~14 days later when tumors were 2 cm in diameter. In some experiments, IL-2 blockade was initiated 1 d prior to tumor cell injection, with injections every 3 d thereafter.

DNFB contact hypersensitivity

Mice were sensitized with 2,4-dinitrofluorobenzene (DNFB) twice on the abdomen (days 0 and 1). After shaving the skin, 0.5% DNFB in 4:1 acetone:olive oil or vehicle control (4:1 acetone:olive oil) was applied to the surface of the skin in a volume of 30 µl per mouse. For elicitation (challenge), 20 µl 0.5% DNFB was applied to the right ear, and 20 µl of vehicle was applied to the left ear. Forty-eight hours after challenge, the change in ear thickness between the affected and unaffected ears was calculated, and cells were isolated from the skin as previously described (Sather *et al.*, 2007).

Bone marrow chimeras

Congenically marked, T cell-depleted bone marrow from WT (CD45.1) and *KLRG1*$^{-/-}$ (CD45.2) mice was injected intravenously into lethally irradiated (1,000 rad) TCRβδ-deficient recipients ($10x10^6$ total bone marrow cells per recipient mouse). The mice were monitored during an 8- to 10-week period of reconstitution by bleeding to ensure appropriate hematopoietic recovery.

Parabiosis

Parabiosis of CD45.2 and CD45.1 congenic mice was performed as previously described (Klonowski *et al.*, 2004). Longitudinal incisions were made along the side of the mouse extending from approximately 1 cm behind the ear to just past the hind limb. Skin was loosened from the connective tissue in the area around the incision, and the fascia of the pair was sutured at the scapulae, thigh, and close to the spine using catgut (Ethicon 4-0 chromic gut sutures, Henry Schein, Denver, PA). The corresponding dorsal edges of skin were joined using 9-mm stainless steel wound clips. Tissues were harvested 14 d after surgery, and the fraction of host-derived $CD4^+Foxp3^+$ Treg cells in each of the indicated tissues was determined by flow cytometry.

Statistical analysis

All data are presented as the mean values ± SEM. Comparisons between groups were analyzed using unpaired or paired Student's t tests or ANOVA with Tukey's post-tests, as appropriate. Statistical significance was established at the levels of $*P \leq 0.05$, $**P \leq 0.005$, and $***P \leq 0.0005$.

CHAPTER 3: Two Populations of Treg Cells with Differential IL-2 Dependence

'Central' and 'effector' Treg cell subsets with distinct homeostatic characteristics

Conventional $CD4^+$ memory cells can be divided into effector memory cells (T_{EM}) that reside in non-lymphoid sites and produce inflammatory mediators and central memory cells (T_{CM}) that recirculate through secondary lymphoid tissues (Sallusto *et al.*, 1999). Similarly, we divided Treg cells into distinct 'central' Treg (cT_R) and 'effector' Treg (eT_R) cell subsets based on their differential expression of CD62L and CD44 (Fig. 3.1). These populations are functionally specialized to control T cell priming or effector function, respectively (Cretney et al., 2013; Huehn et al., 2005), and accordingly, $CD44^{lo}CD62L^{hi}$ cT_R cells actively recirculated through secondary lymphoid tissues, whereas $CD44^{hi}CD62L^{lo}$ eT_R cells showed limited recirculation and were the predominant Treg cell population in non-lymphoid tissues such as the liver and intestines (Fig. 3.2A, B). In addition, eT_R cells were highly enriched for the expression of adhesion and chemoattractant receptors required for migration to non-lymphoid tissues such as CXCR3, CD103, and P-selectin ligand, and for surface markers associated with cellular activation, such as CD69, KLRG1, and ICOS (Fig. 3.3A and data not shown). In contrast, expression of the transcription factor Helios, which, along with Neuropilin-1, is preferentially expressed by thymus-derived Treg cells (Thornton *et al.*, 2010; Yadav *et al.*, 2012), was identical in cT_R and eT_R cells (Fig. 3.3B).

Regarding proliferation, which was assessed by the incorporation of 5-bromo-2'deoxyuridine (Brdu) or by expression of the cell cycle-associated antigen Ki-67, much greater levels were observed in eT_R cells than cT_R cells (Fig. 3.4A and data not shown). By contrast, eT_R cells expressed significantly less CD25 and lower levels of

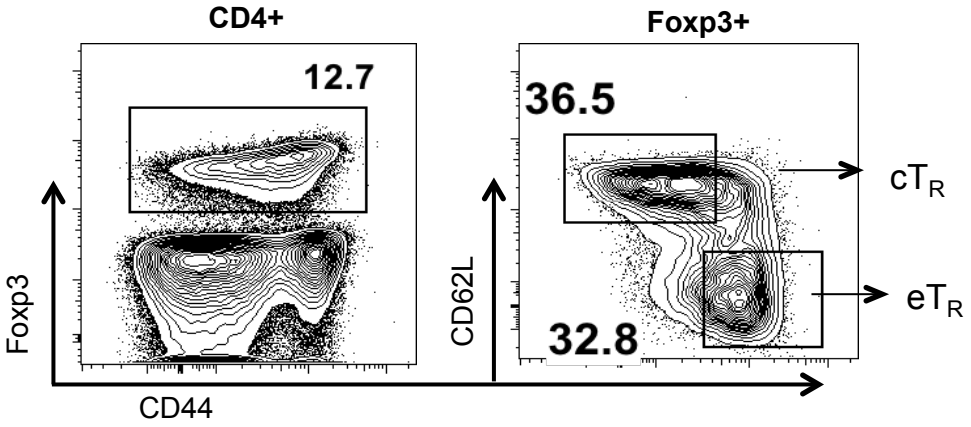

Figure 3.1. CD44 and CD62L define two populations of central and effector Treg cells.
Spleen cells from WT mice were isolated, and CD4+ T cells were analyzed for Foxp3, CD44, and CD62L expression by flow cytometry. Gates (right plot) show the cT_R ($CD44^{lo}CD62L^{hi}$) and eT_R ($CD44^{hi}CD62L^{lo}$) frequencies of total CD4+Foxp3+ cells.

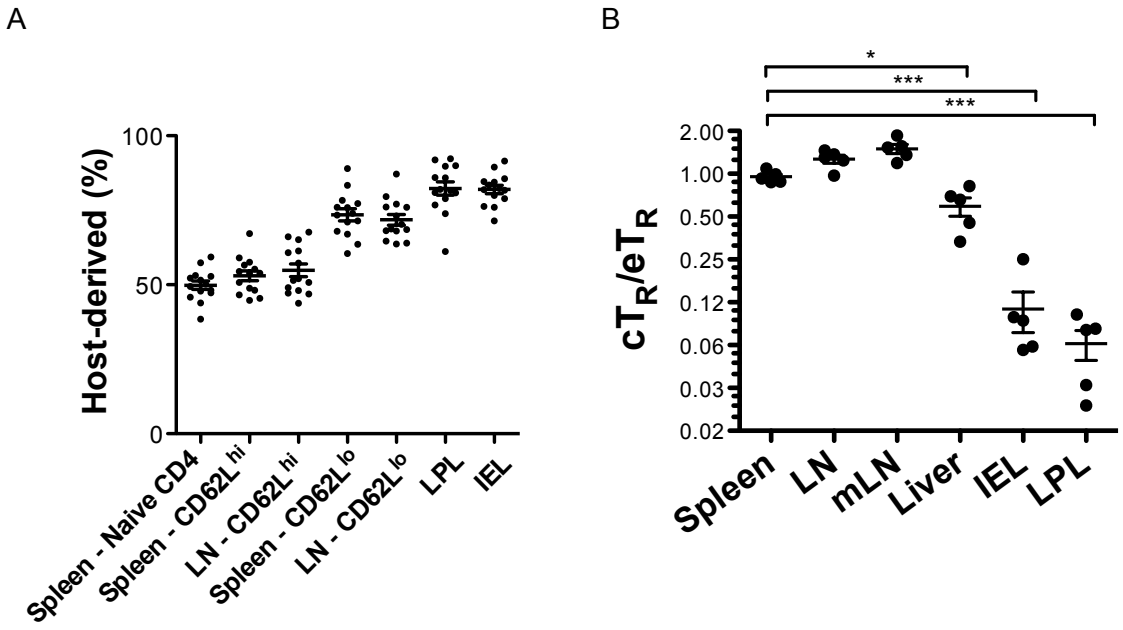

Figure 3.2. eT_R cells show limited recirculation and reside in peripheral tissues.

(A) The frequencies of host-derived cells in CD45.1:CD45.2 parabiotic mice are shown for naïve $CD4^+Foxp3^-CD44^{lo}$, $CD62L^{hi}$ cT_R, and $CD62L^{lo}$ eT_R cells in the spleen and LN, as well as total Treg cells in the intestinal LPL and IEL, after a 14-d period of parabiosis (n=14) . (B) Ratio of cT_R to eT_R cells in the indicated tissues (n=5 WT mice).

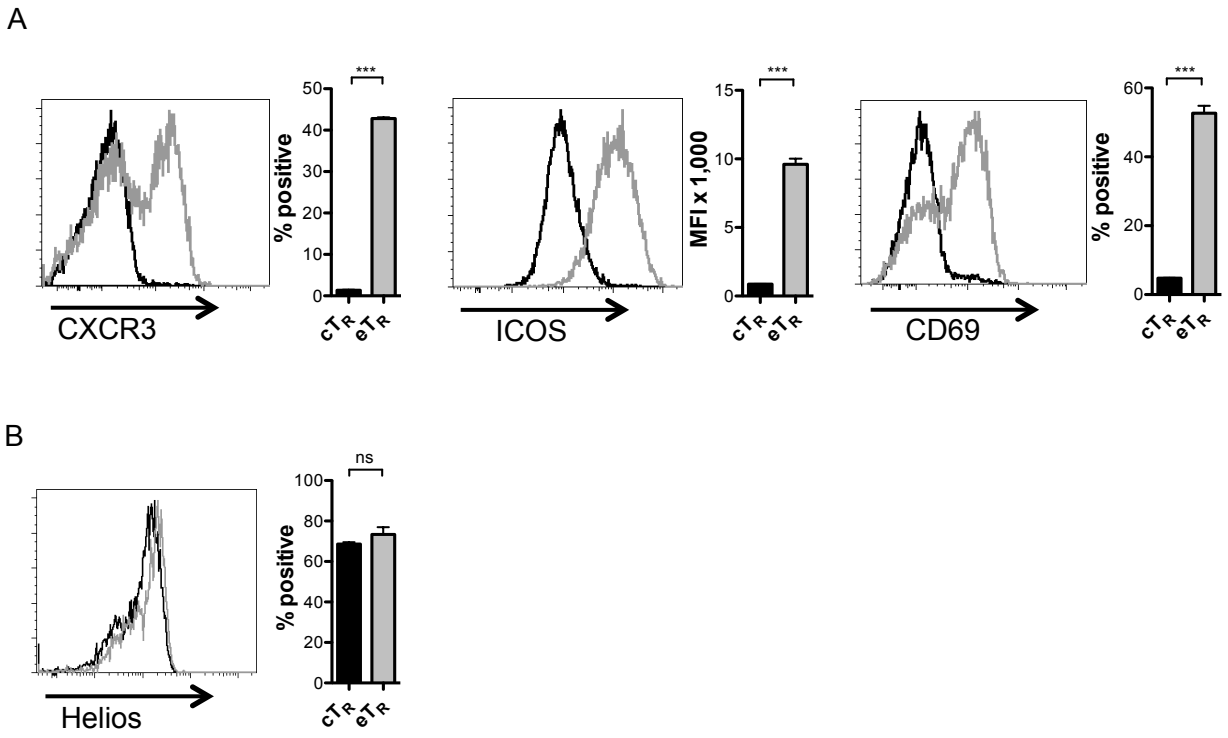

Figure 3.3. cT_R and eT_R cells show diverse activation profiles but similar Helios expression.
(A) Splenic cT_R (black) and eT_R (grey) cells were analyzed by flow cytometry (n=3 mice) for expression of (A) the indicated homing and activation markers and (B) Helios.

the pro-survival factors Bcl2 and *Mcl1* than cT_R cells, and eT_R cells were highly susceptible to spontaneous apoptosis during short-term *in vitro* culture (Fig. 3.4B-E). Thus, whereas cT_R cells are quiescent and appear to be long-lived, eT_R cells are undergoing rapid proliferation *in vivo*, which is balanced by a high rate of apoptotic cell death.

Thymic cT_R generation and peripheral eT_R conversion

Although the majority of cT_R and eT_R cells demonstrated a phenotype indicative of thymic origin, it remained unclear whether these cells are generated as unique populations in the thymus or whether the separation of these 2 subsets occurs in the periphery secondary to environmental cues. To compare the phenotypes of thymic and peripheral Treg cells, we utilized transgenic mice expressing GFP under control of the RAG2 promoter to distinguish true developing thymic Treg cells from GFP^- Treg cells that have migrated from the periphery back into the thymus. Analysis of sorted $CD4^+CD8^-GFP^+$ thymocytes revealed that developing Treg cells were uniformly $Ki\text{-}67^-ICOS^-$ cT_R cells, whereas eT_R cells were only found among the GFP^- cells (Fig. 3.5A, B). Because detectable GFP protein remains in cells for ~2 weeks after exit from the thymus (Boursalian *et al.*, 2004), we also used RAG2-GFP mice to identify and characterize recent thymic emigrants (RTEs) in the periphery. This analysis revealed that eT_R cells were rare among GFP^+ RTEs but greatly enriched among GFP^- cells (Fig. 3.6A, B). To further address the developmental relationship between cT_R and eT_R cells, we evaluated the proliferation and phenotype of sorted cT_R and eT_R cells 15 days after transfer into congenically disparate recipients. Indeed, a substantial fraction of the transferred cT_R cells had become $CD44^{hi}CD62L^{lo}$ eT_R cells, and acquisition of the eT_R phenotype was associated with extensive proliferation; by contrast, transferred eT_R cells were phenotypically stable and retained their

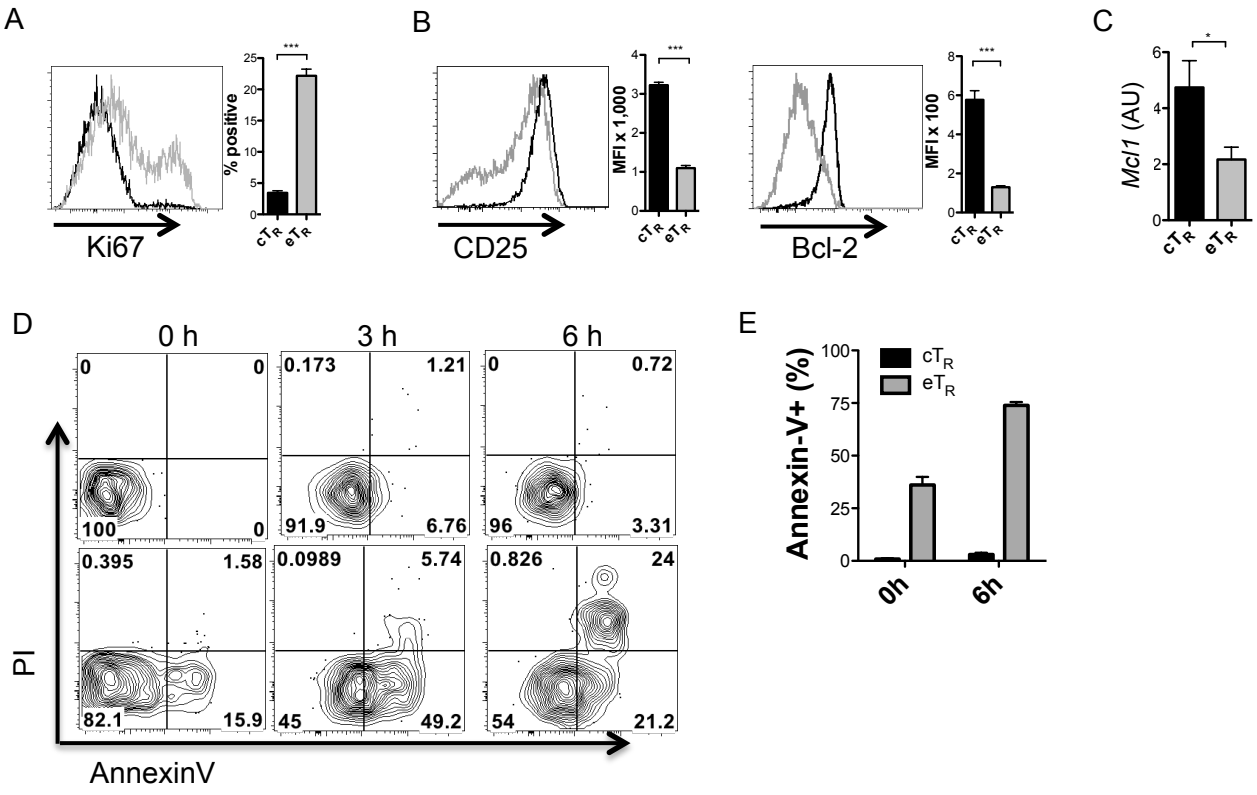

Figure 3.4. eT_R cells are highly proliferative and short-lived.
(A) Splenic cT_R (black) and eT_R (grey) cells were analyzed by flow cytometry (n=3 mice) for expression of (A) Ki-67 and (B) CD25 and Bcl-2. Sorted splenic cT_R (black) and eT_R (grey) cells were analyzed by qPCR for expression of (C) *Mcl1* (n=3 replicates). (D) Representative flow cytometry analysis of AnnexinV binding and propidium iodide (PI) labeling in gated splenic cT_R (top) and eT_R (bottom) cells following *in vitro* culture for the indicated times. (E) The frequencies of Annexin-V-binding splenic cT_R and eT_R cells were determined by flow cytometry directly *ex vivo* and following 6 h of culture (n=3 mice).

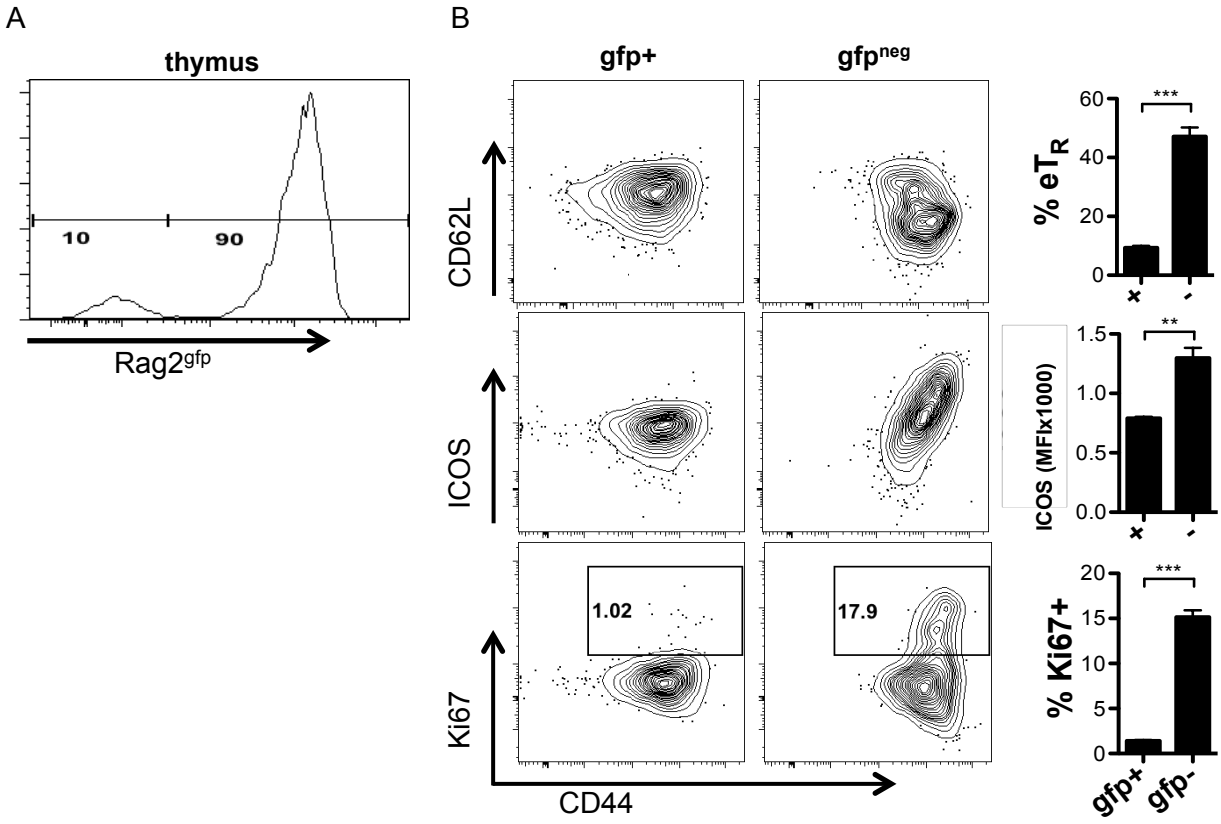

Figure 3.5. Thymic Tregs are predominantly cT_R cells.
(A) Thymic CD4+ cells from Rag2^{gfp} mice were FACS-sorted according to GFP expression. (B) Sorted thymic gfp+/- cells were analyzed for Foxp3, CD44, CD62L, ICOS, and Ki-67 expression by flow cytometry. The middle plots are gated on Foxp3+GFP+ or Foxp3+GFP- cells, as indicated. The bar graphs (at right) show the percentage of eT_R cells (top), the MFI of ICOS expression (middle), and the percentage of Ki67+ cells (bottom) among gfp+ and gfp- cells (n=5 Rag2^{gfp} mice).

A

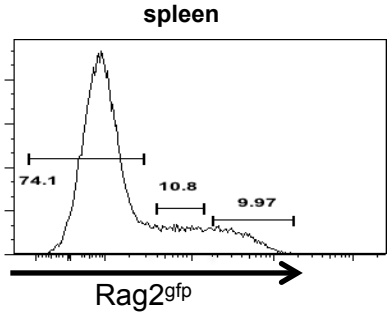

B

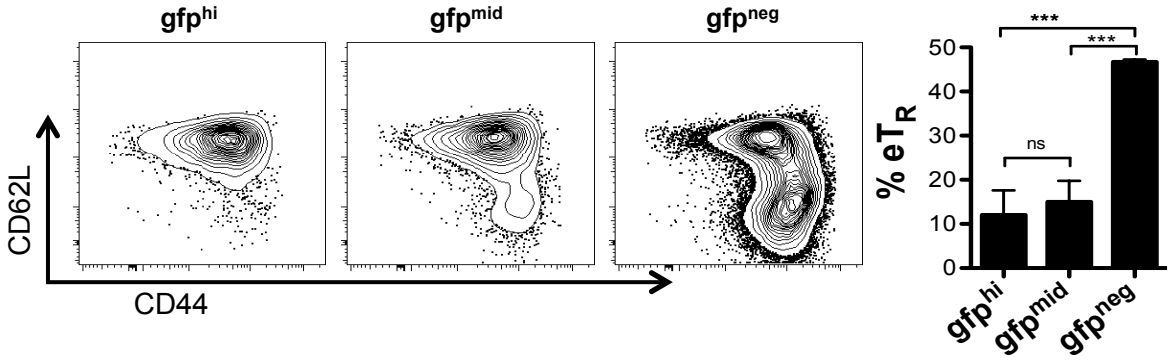

Figure 3.6. eT_R cells are generated in the periphery after exit from the thymus.
(A) Splenic CD4+ cells from $Rag2^{gfp}$ mice were FACS-sorted according to GFP expression. (B) Sorted splenic gfp^{hi}, gfp^{mid} and gfp^{neg} cells were analyzed for Foxp3, CD4 and CD62L by flow cytometry. The bar graph at the right show the percentage of eT_R cells among total Foxp3+ cells.

$CD44^{hi}CD62L^{lo}$ phenotype (Fig. 3.7). Together, these data are consistent with the notion that Treg cells emerge from the thymus as cT_R cells and that phenotypically stable eT_R cells subsequently differentiate from cT_R precursors in the periphery.

cT_R cells selectively require IL-2 *in vivo*

The dramatic differences in the phenotype, localization, and behavior of the cT_R and eT_R cell populations suggest that unique sets of homeostatic signals control their proliferation and survival. In particular, reduced expression of Mcl1, Bcl2, and CD25 in eT_R cells is strongly indicative of a lack of ongoing IL-2 signaling in this population (Tang *et al.*, 2008; Malek and Ashwell, 1985; Pierson *et al.*, 2013). Indeed, direct *ex vivo* assessment of Stat5 phosphorylation (pStat5) revealed that IL-2 signaling was largely restricted to the $CD44^{lo}CD62L^{hi}$ cT_R population and was not associated with highly proliferative eT_R cells (Fig. 3.8). Furthermore, inhibition of IL-2 signaling *in vivo* through loss of CD25 or IL-2 in *Il2ra*$^{-/-}$ or *Il2*$^{-/-}$ mice, or through acute neutralization of IL-2 using blocking antibodies, abolished detectable Stat5 phosphorylation in Treg cells (Fig. 3.9) and led to a selective decrease in both the frequency and number of cT_R cells without significantly impacting the abundance or proliferation of eT_R cells in the spleen, lymph nodes, or non-lymphoid tissues such as the intestinal lamina propria (Fig. 3.10A-C). To determine whether IL-2 is required for eT_R maintenance and/or proliferation in a competitive setting, we co-transferred sorted $CD4^+Foxp3^+$ Treg cells from WT and *Il2ra*$^{-/-}$ mice into congenically marked WT recipients and examined the recovery of cells from the spleen 1 week later. Surprisingly, the recovery of *Il2ra*$^{-/-}$ Treg cells was nearly equivalent to that of co-transferred WT cells (Fig. 3.11A, average ratio of WT:*Il2ra*$^{-/-}$ Treg cells recovered = 1.32 +/- 0.13, n=6 mice analyzed in 3 separate experiments), indicating that these cells could effectively compete with WT cells for IL-2-independent growth and survival factors *in vivo*. Additionally, incorporation of BrdU was identical in

transferred WT and *Il2ra*$^{-/-}$ Treg cells (data not shown). Because differences in activation and environment between cells isolated from *Il2ra*$^{-/-}$ and WT mice may influence their behavior upon transfer, we also examined the proliferation of sorted eT_R cells from WT mice transferred into a-IL-2-treated recipients; however, we found that blockade of IL-2 had no discernible effect on the proliferation of transferred eT_R cells in these recipients (Fig. 3.11B). Taken together, these data show that although required for the maintenance of cT_R phenotype cells, eT_R cells do not actively respond to IL-2 *in vivo*, and loss of IL-2 signaling does not impair eT_R cell homeostatic maintenance or proliferation, even when placed in direct competition with IL-2-responsive cells.

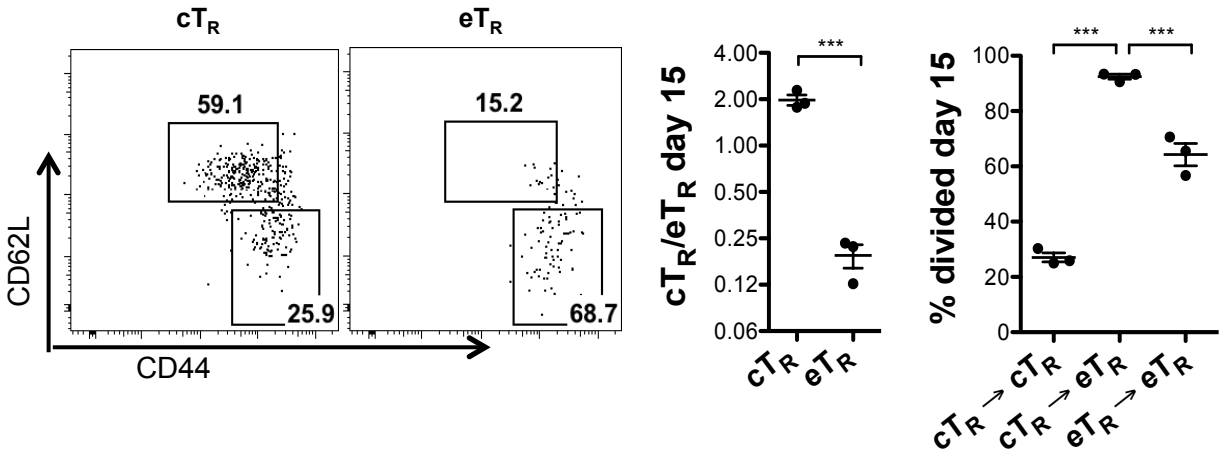

Figure 3.7. Terminally differentiated eT_R cells are generated from cT_R cells in the periphery.
FACS-sorted cT_R or eT_R cells from WT mice ($2x10^5$ cells) were adoptively transferred to congenic WT recipient mice (n=3 per group) and analyzed 15 days later for any changes in CD44 vs. CD62L phenotype (left plots), the resulting cT_R to eT_R cell ratio (middle), and the percent divided based on staining with the eFluor670 cell proliferation dye (right). Legend for the y-axis on the right graph: cT_R➔cT_R, cT_R cells that stayed cT_R cells; cT_R➔eT_R, cT_R cells that differentiated into eT_R cells; and eT_R➔eT_R, eT_R cells that stayed eT_R cells.

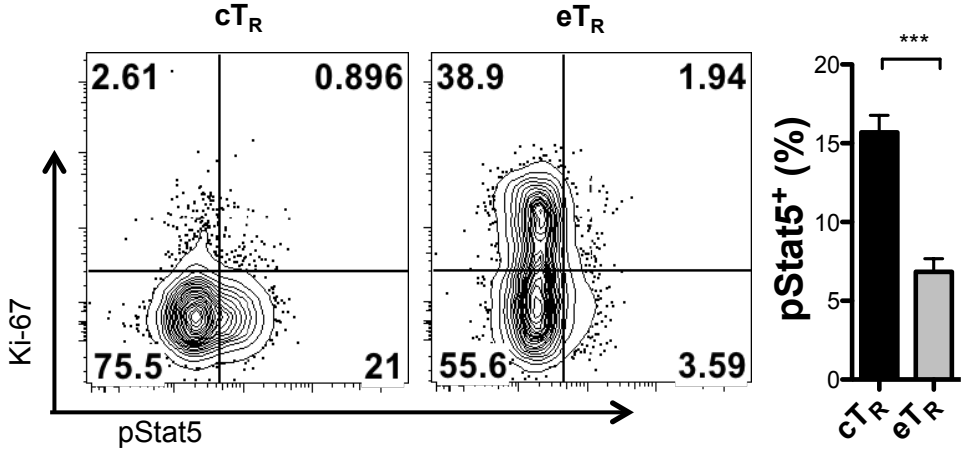

Figure 3.8. IL-2 signaling occurs in cT_R cells and is not associated with proliferation.
Spleen cells from WT mice were isolated, and CD4+ T cells were analyzed directly *ex vivo* for Foxp3, CD44, CD62L, Ki-67, and pStat5 expression by flow cytometry. The plots show pStat5 and Ki-67 expression among gated cT_R and eT_R cells, and the bar chart shows the frequency of pStat5+ cells among gated eT_R and cT_R cells (n=3 mice).

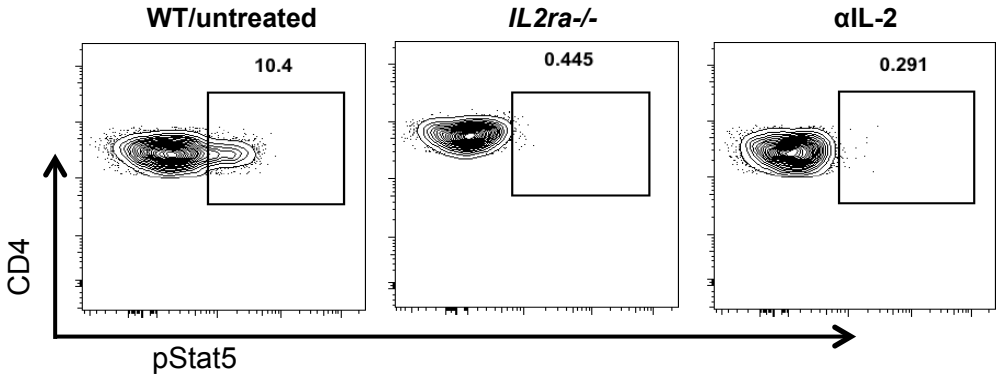

Figure 3.9. IL-2 signaling is blocked in the absence of CD25 or following treatment with anti-IL-2 antibodies.
Representative *ex vivo* pStat5 staining in gated Foxp3+ cells from WT/ untreated, *Il2ra-/-* and 2-week αIL-2-treated mice. The IL-2-blocked mice received 1 injection of anti-IL-2 antibodies, and the staining was performed 3 days later.

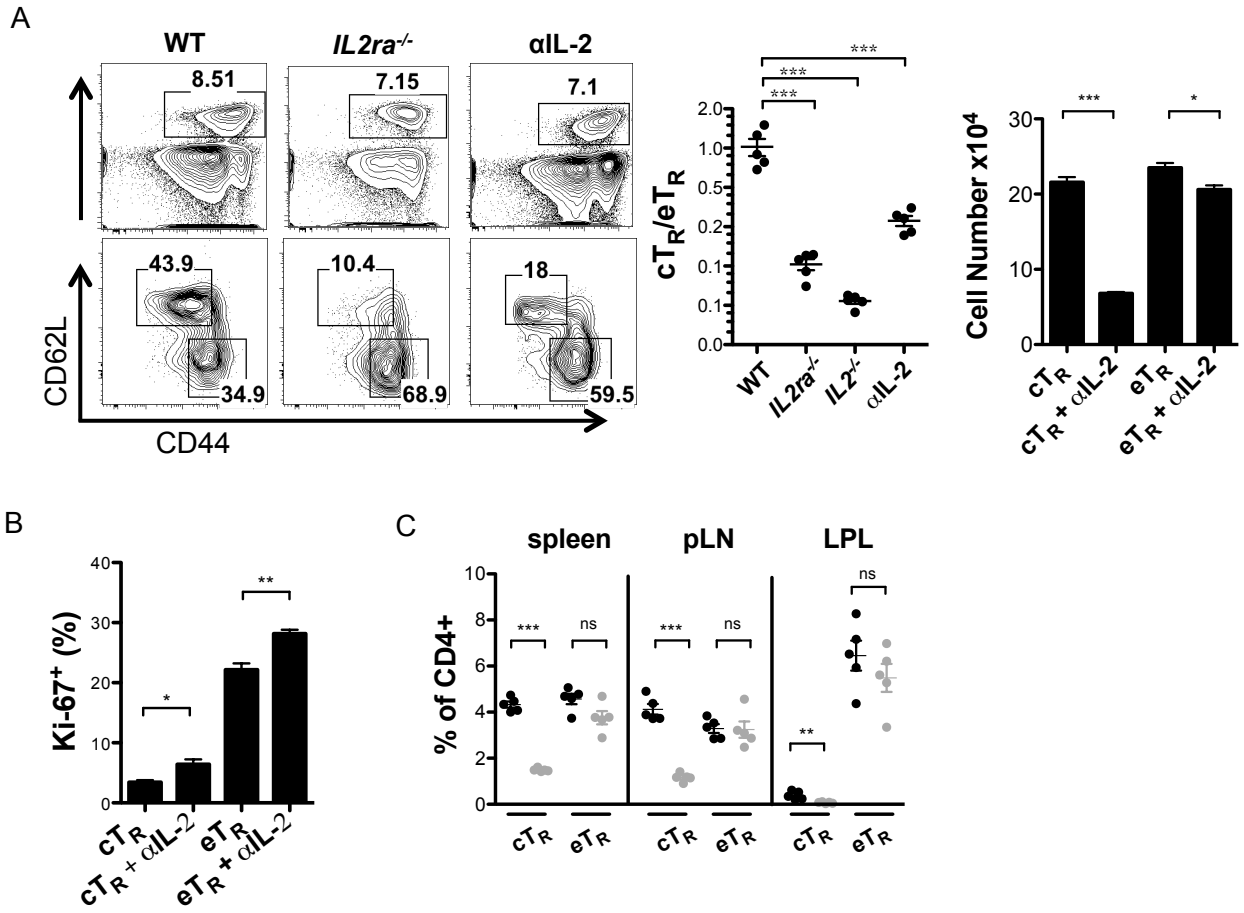

Figure 3.10. cT_R cells are uniquely dependent on IL-2 signaling *in vivo*. Spleen cells from WT, *Il2ra*$^{-/-}$, Il2$^{-/-}$, and anti(α)-IL-2-treated mice were isolated, and CD4+ T cells were analyzed by flow cytometry for Foxp3, CD44, CD62L and Ki-67 expression. (A) The left plots show representative frequencies of Foxp3$^+$, cT_R, and eT_R cells in WT, *Il2ra*$^{-/-}$, and 2-week αIL-2-treated mice, the middle chart shows the cT_R to eT_R cell ratios for WT, *Il2ra*$^{-/-}$, Il2$^{-/-}$, and 2-week αIL-2-treated mice (n=4-5 mice per group), and bar graph shows total cell number for the indicated groups. (B). The frequency of Ki67$^+$ cT_R and eT_R cells in control- and αIL-2-treated mice is shown in the bar chart (n=5 per group). (C) The frequencies of cT_R and eT_R cells among CD4$^+$ cells were measured for the indicated tissue sites following 2-week treatment with control (black circles) or α-IL-2 antibodies (grey circles). Each symbol represents data from 1 animal (n=5 total).

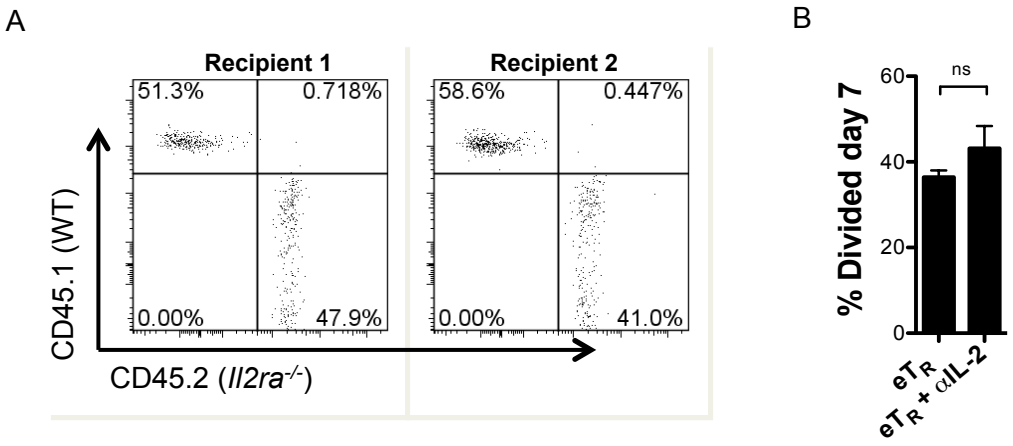

Figure 3.11. eT_R cells can survive and proliferate in the absence of IL-2.

(A) FACs-sorted CD4$^+$Foxp3^{gfp+} T cells from CD45.1$^+$ B6.SJL and CD45.2$^+$ *Il2ra*$^{-/-}$ mice were co-transferred into CD45.2$^+$Foxp3^{gfp-} recipients, and the flow cytometry analysis of CD45.1 and CD45.1 expression by CD4$^+$Foxp3^{gfp+} Treg cells in the spleens of 2 representative recipient animals 7 days after transfer is shown. Results are representative of 6 animals analyzed in 3 independent experiments. (B) FACS-sorted eT_R cells ($2x10^5$) were labeled with the eFluor670 cell proliferation dye and adoptively transferred into congenic recipient mice, with 1 group receiving αIL-2 injections on days -1, 2, and 5 (n=3 mice per group). Recovered cells from the spleen were analyzed by flow cytometry for eFluor670 dye dilution (as a read-out of proliferation) on day 7 post-transfer.

CHAPTER 4: CCR7 Expression Controls the Spatial Regulation of IL-2 Signaling

Paracrine IL-2 signaling is spatially regulated

Both cT_R and eT_R cells were highly responsive to exogenous IL-2 *in vitro* and *in vivo* (Fig. 4.1A, B), indicating that despite reduced surface CD25 expression, the lack of IL-2 signaling in eT_R cells is not due to an intrinsic inability to respond to this cytokine. We therefore tested whether the enhanced IL-2 signaling in cT_R cells *in vivo* was due to their ability to localize to specific environments that facilitate paracrine IL-2 signaling to regulatory T cells. For this, we examined the distribution and homeostasis of Treg cells in the spleen due to the similar number of cT_R and eT_R cells in this organ.

The spleen has a complex structure, with T and B cells predominantly found in the highly organized splenic white pulp (WP), which is surrounded by the B cell-rich marginal zone (MZ) and the macrophage/granulocyte-rich red pulp (RP). Although the majority of splenic Foxp3$^+$ Treg cells were localized within the WP T cell zones, a significant fraction was found outside of the MAdCAM-1$^+$ marginal sinus in the MZ and RP (Fig. 4.2). However, assessing the location of IL-2 signaling in Treg cells histologically, we found that pStat5$^+$ Treg cells were found almost exclusively inside of the WP T cell zones (Fig. 4.3). Similarly, pStat5$^+$ Treg cells were readily observed within the T cell zones in both lymph nodes and Peyer's patches, whereas the frequency of pStat5$^+$ Treg cells in the small intestinal lamina propria was low (<10%) and comparable to that observed in splenic Treg cells in the MZ/RP (Fig. 4.4). To further quantify where IL-2 signaling takes place within the spleen, we intravenously injected mice with phycoerythrin (PE)-labeled anti-CD4 antibody, which labels cells in the RP/MZ but is excluded from the T cell zones in the WP due to

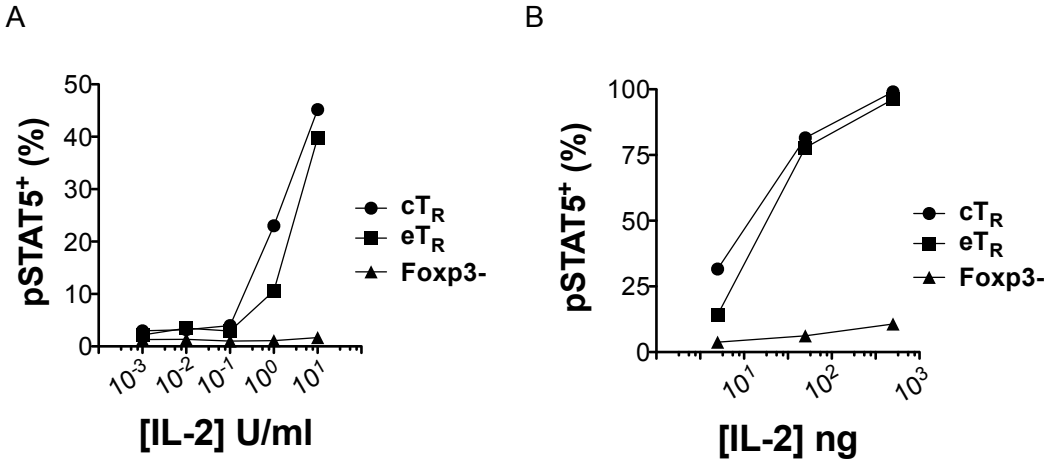

Figure 4.1. cT_R and eT_R cells are equally capable of responding to IL-2.
(A) Splenic CD4+ T cells were analyzed by flow cytometry for Foxp3, CD44, CD62L, and pStat5 expression. The average percentage of $pStat5^+$ cells among gated cT_R, eT_R, and $CD4^+Foxp3^+$ cells following treatment with the indicated amounts of IL-2 *in vitro* (A) or *in vivo* (B) is shown (the average of 3 data points is plotted).

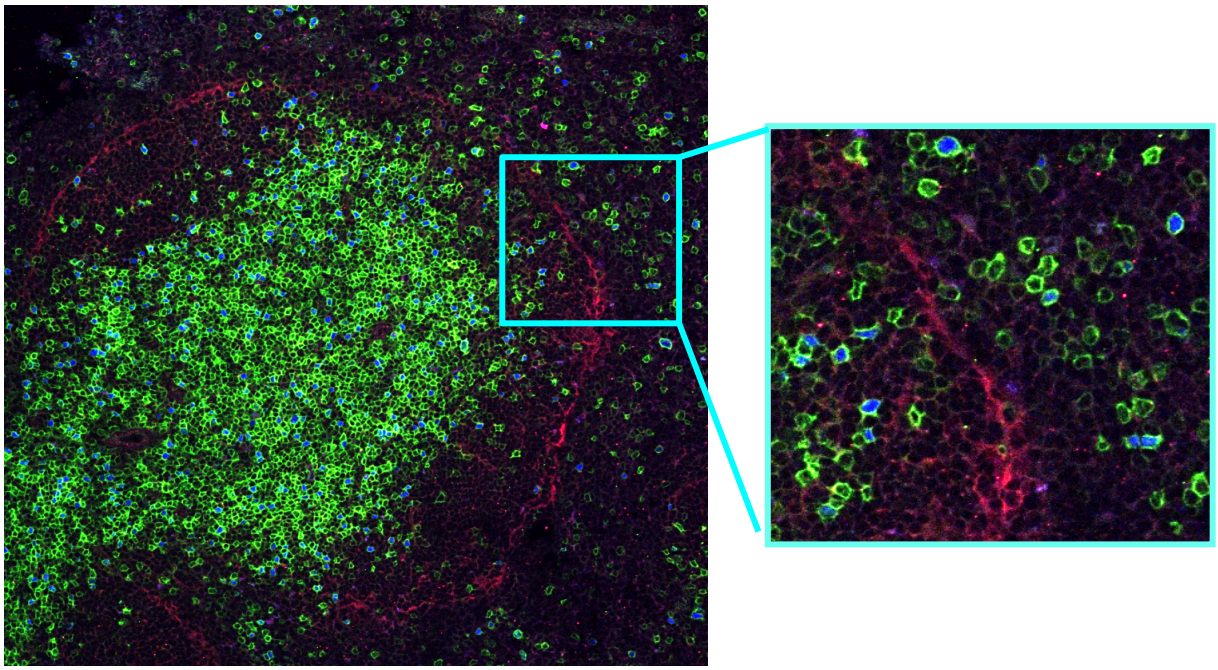

Figure 4.2. Treg cells are located both inside and outside of the marginal sinus.
Representative confocal image of the spleen showing $CD5^{+}Foxp3^{+}$ cells in both the WP T cell zones within the $MadCAM\text{-}1^{+}$ marginal sinus and in the MZ/RP outside of the marginal sinus.

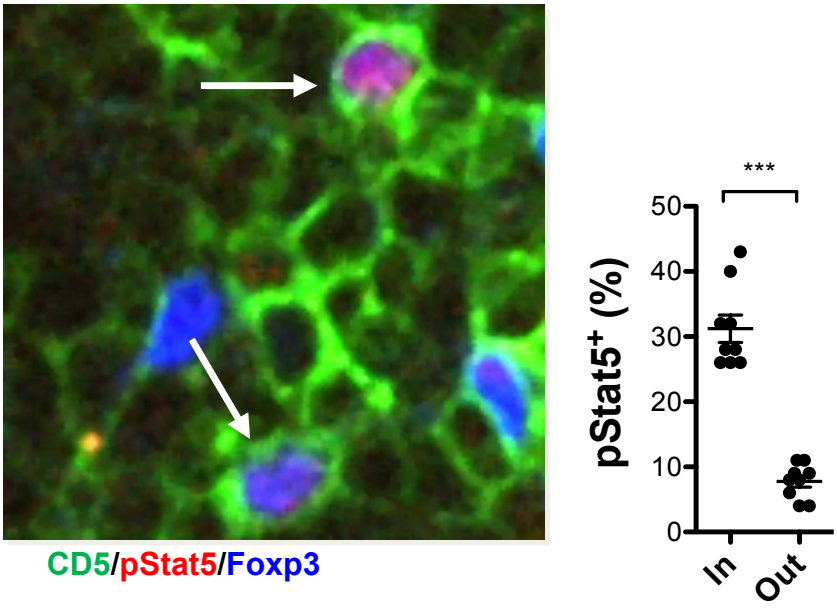

Figure 4.3. IL-2 signaling occurs within the T cell zones of the spleen. Representative confocal image showing the splenic co-localization of Foxp3 and pStat5 (dual-positive cells are indicated with arrows) . The percentage of Treg cells located inside or outside of the T cell zones that were pStat5^{+} is indicated graphically (n=9 fields from 3 mice).

A

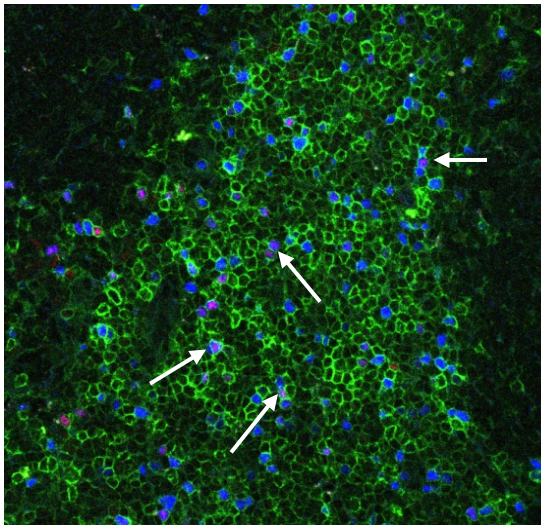

CD5/pStat5/Foxp3

B

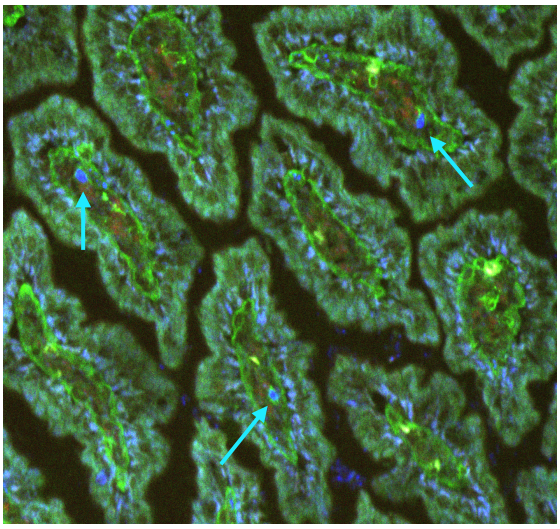

CD5/pStat5/Foxp3

Figure 4.4. IL-2 signaling is common in lymphoid tissues but rare in non-lymphoid tissues.
Representative confocal images of the Peyer's patch (A) and small intestine (B) stained for CD5, pStat5, and Foxp3 as indicated. The white arrows (A) denote $CD5^{+}Foxp3^{+}pStat5^{+}$ cells, whereas the blue arrows (B) indicate $CD5^{+}Foxp3^{+}pStat5^{-}$ cells. For the small intestine, a total of 5 $pStat5^{+}$ cells were observed among 54 total Treg cells identified in sections from 3 separate mice.

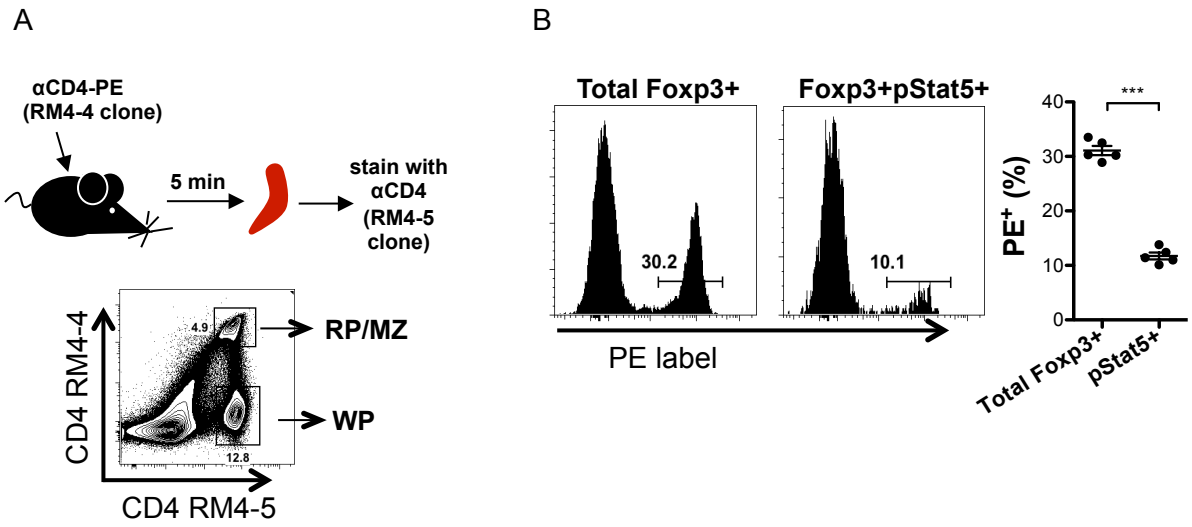

Figure 4.5. pStat5$^+$ cells are shielded from the circulation.
For *in vivo* PE labeling, αCD4-PE antibody (RM4-4 clone) was injected intravenously, and spleens were harvested 5 min post-injection. Splenocytes were examined by flow cytometry after staining with an RM4-5 clone αCD4 antibody. (A) The representative flow cytometry plot shows the dual-labeled RP/MZ and single-labeled WP CD4$^+$ T cells. (B) After *in vivo* PE labeling (n=5 mice), splenocytes were analyzed by flow cytometry for CD4, Foxp3, and pStat5 expression. The histograms (left) and chart (right) show the frequencies of total Foxp3$^+$ and Foxp3$^+$pStat5$^+$ cells labeled *in vivo* with anti-CD4 PE.

the relatively impermeant marginal sinus (Cinamon *et al.*, 2008). Following tissue harvest, we compared Stat5 phosphorylation among WP and RP/MZ Treg cells, and consistent with our confocal analyses, pStat5^{+} Treg cells were found predominantly among unlabeled WP cells (Fig. 4.5). Thus, IL-2 signaling is not only restricted to cT_R cells but also is strongly associated with Treg cell localization in the organized T cell zones of secondary lymphoid organs.

CCR7 guides Treg cells to sources of IL-2

The chemokine receptor CCR7 directs T cell migration to and within the secondary lymphoid tissues and could thereby bring Treg cells into close juxtaposition with IL-2-producing T cells (Forster *et al.*, 1999). Indeed, expression of CCR7 by eT_R cells was significantly lower than on cT_R cells (Fig. 4.6). Thus, we hypothesized that selective expression of CCR7 gives cT_R cells preferential access to IL-2 and is therefore required to maintain the homeostatic balance between cT_R and eT_R cells. Consistent with this, Treg cells in *Ccr7*$^{-/-}$ mice strongly resembled the 'IL-2-starved' Treg cells observed in *Il2ra*$^{-/-}$ and anti(α)-IL-2-treated mice, with a selective decrease in cT_R cells and reduced expression of CD25 and Bcl2 compared to age-matched WT controls (Fig. 4.7). Moreover, Stat5 phosphorylation was dramatically reduced in *Ccr7*$^{-/-}$ Treg cells, whereas Ki-67 expression was slightly elevated (Fig. 4.8). CCR7 controls the migration of multiple cell types, including naïve T cells, central memory T cells, and activated DCs (Forster *et al.*, 2008). However, sorted *Ccr7*$^{-/-}$ cT_R cells failed to efficiently enter the WP or phosphorylate Stat5 upon adoptive transfer into WT hosts (Fig. 4.9A), demonstrating a cell-intrinsic defect in the ability of *Ccr7*$^{-/-}$ Treg cells to access sites of paracrine IL-2 signaling *in vivo*. Because the immune dysregulation present in *Ccr7*$^{-/-}$ mice could potentially affect the behavior of transferred cells, we took an alternative approach and inhibited chemoattractant receptor signaling in WT Treg cells by treatment with pertussis toxin

(ptx) *in vitro* prior to transfer into congenically distinct recipients. As we had observed for CCR7-deficient Treg cells, ptx-treated Treg cells localized effectively to the spleen but showed dramatically reduced Stat5 phosphorylation (Fig. 4.9B). Although ptx inhibits signaling through all G_ai-linked chemoattractant receptors and is not a specific inhibitor of CCR7, this result shows that CCR-mediated migration of Treg cells within the spleen is important for WT Treg cells to properly access IL-2, and together these data demonstrate that CCR7 guides cT_R cells to an IL-2 signaling 'niche', thereby functioning to control the balance of cT_R and eT_R cells *in vivo*.

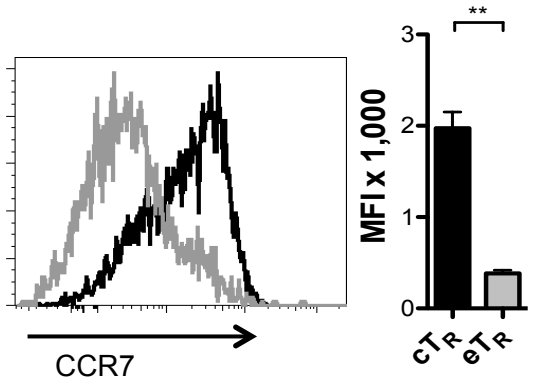

Figure 4.6. CCR7 expression is significantly higher on cT_R cells.
Spleen cells were isolated, and CD4+ cells were analyzed for Foxp3, CD44, CD62L, and CCR7 expression by flow cytometry. CCR7 staining was performed using a CCL19-human IgGFc fusion protein. The bar chart shows the MFI of CCR7 among cT_R (black) and eT_R (grey) cells (n=3 mice).

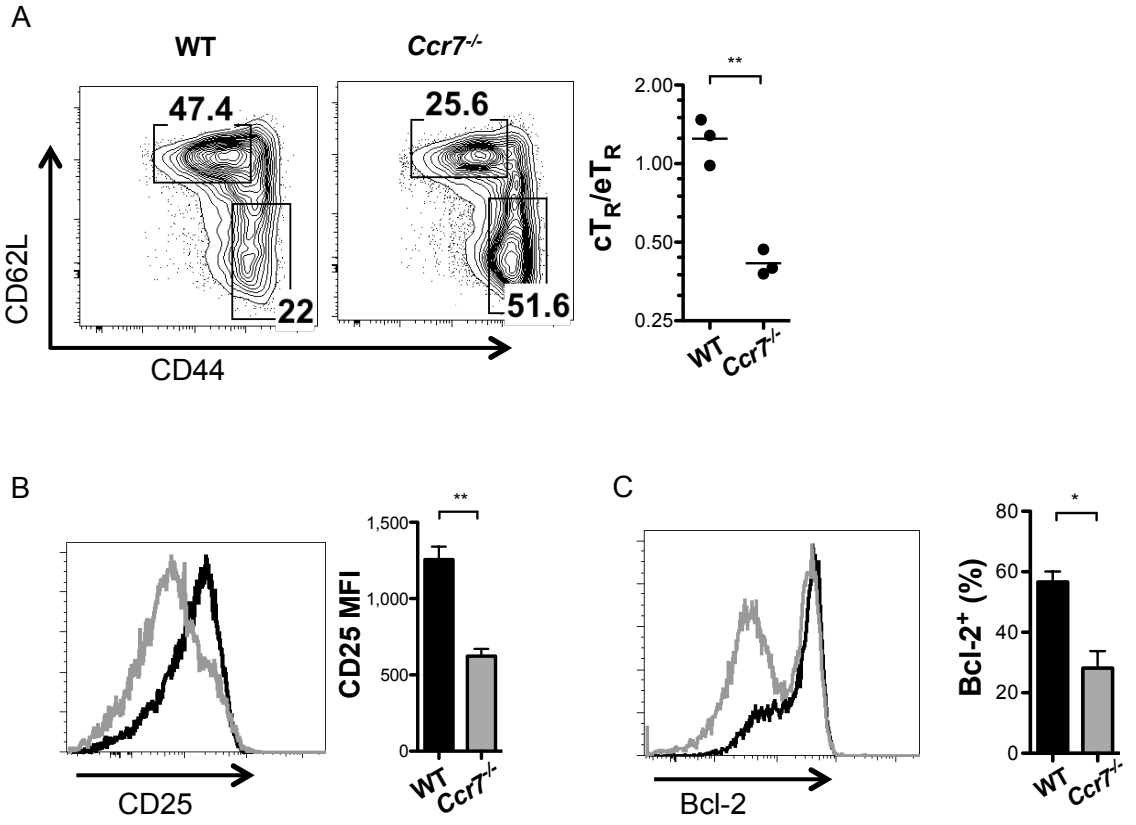

Figure 4.7. *Ccr7*$^{-/-}$ mice show a selective reduction in cT_R cells. Spleen cells from WT and *Ccr7*$^{-/-}$ mice were isolated, and CD4+ cells were analyzed by flow cytometry for Foxp3, CD44, CD62L, CD25 and Bcl-2 expression directly *ex vivo*. (A) The plots show representative frequencies of cT_R and eT_R cells, and the chart shows the cT_R to eT_R cell ratios in WT and *Ccr7*$^{-/-}$ mice (n=3 per group). (B,C) The histograms and bar graphs show (B) CD25 and (C) Bcl-2 expression among gated Foxp3+ cells in WT (black) vs. *Ccr7*$^{-/-}$ (grey) mice (n=3 per group).

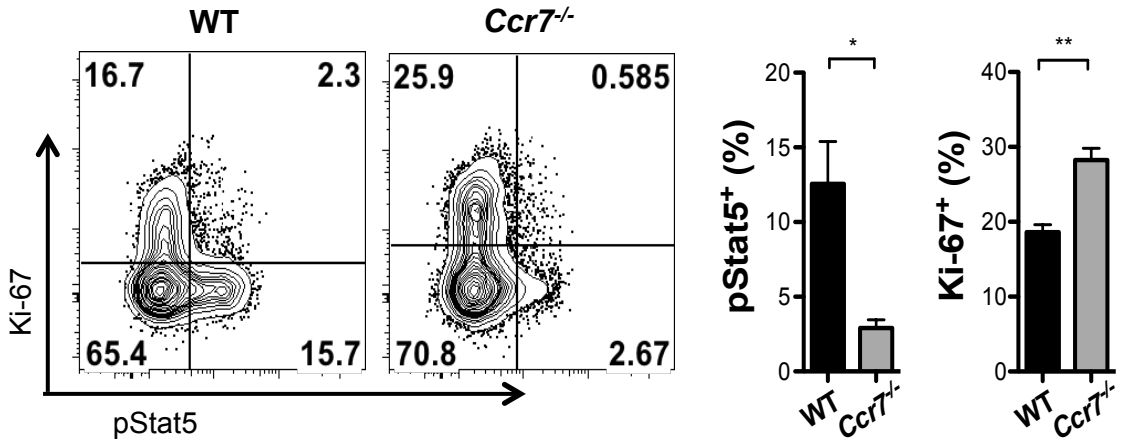

Figure 4.8. CCR7 is required for maximal IL-2 responsiveness.
The plots show representative flow cytometric staining for pStat5 and Ki-67 expression directly *ex vivo* in gated Treg cells from WT and *Ccr7*$^{-/-}$ mice, and the bar charts show the percentage of Treg cells expressing pStat5 (left) or Ki-67 (right) in each group (n=3 each).

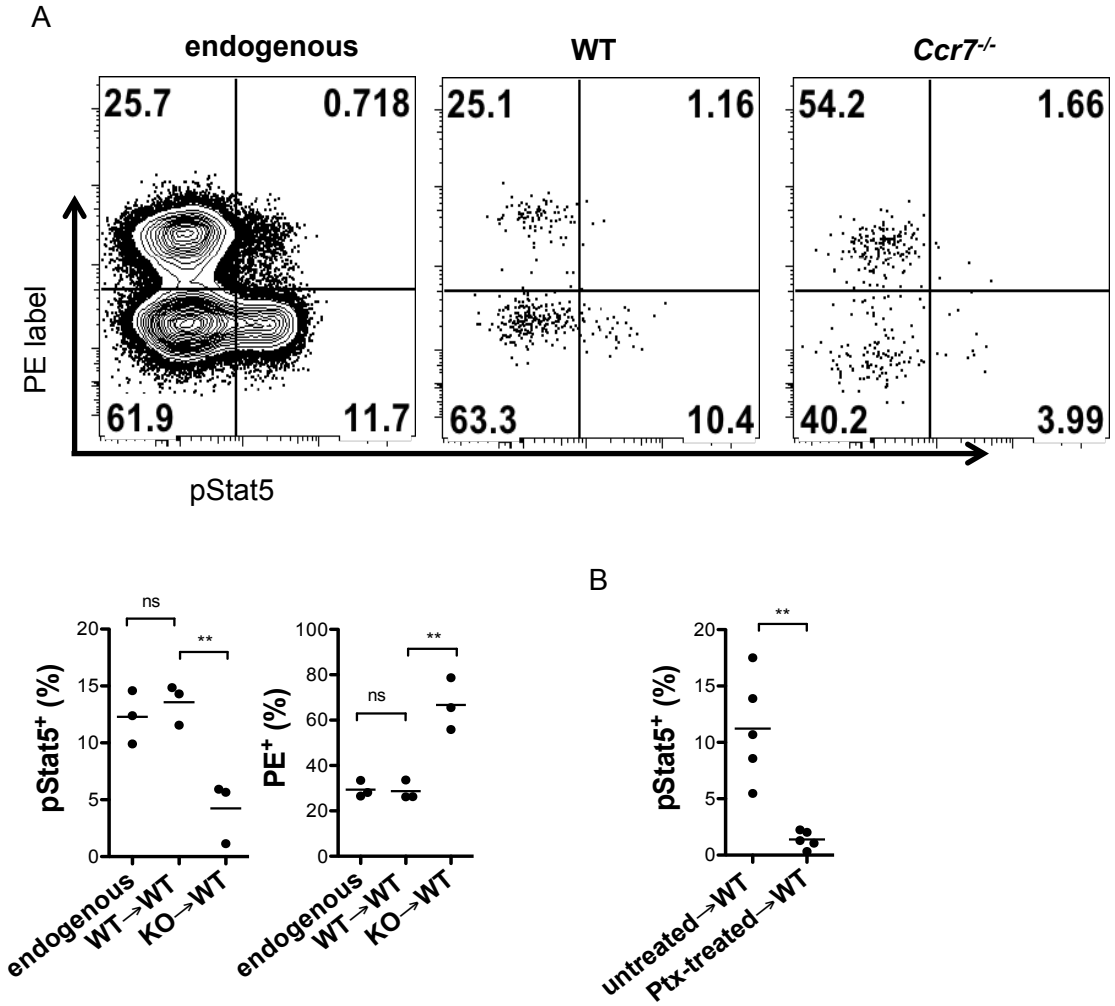

Figure 4.9. Cell-intrinsic $G_{\alpha}i$ and CCR7 signaling is required for cT_R cells to access IL-2 *in vivo*.

(A) FACS-sorted WT or *Ccr7*$^{-/-}$ cT_R cells ($2x10^5$) were adoptively transferred into congenically disparate hosts, and cell localization within the spleen (following *in vivo* PE labeling) and Stat5 phosphorylation were examined by flow cytometry for endogenous Treg cells and Treg cells recovered at 36 h post-transfer. The plots on the left show representative flow cytometry staining for pStat5 and *in vivo*-labeled CD4-PE. The charts on the bottom show the percentage of Treg cells in each group demonstrating positive staining for pStat5 (left) and the *in vivo* CD4-PE label. Y-axis legend: WTèWT, WT cT_R cells injected into WT recipients (n=3); KOèWT, *Ccr7*$^{-/-}$ cT_R cells injected into WT recipients (n=3). (B) Stat5 phosphorylation was measured by flow cytometry in WT Treg cells that were left untreated or treated for 2 h *in vitro* with pertussis toxin (Ptx) and then transferred into congenic recipient mice for 36 h prior to analysis.

CHAPTER 5: The Promotion and Maintenance of IL-2-independent Treg Cells

eT_R cell abundance is controlled by DCs and is ICOS-dependent

Treg cell abundance is tightly linked to the number of antigen-presenting DCs (Darrasse-Jeze *et al.*, 2009). Although this may be due to the ability of DCs to directly present relevant self-antigens and provide important co-stimulatory signals to self-reactive Treg cells, it could also be secondary to the ability of DCs to trigger IL-2 production from conventional $Foxp3^-$ T cells. To distinguish between these possibilities, we examined the homeostasis of cT_R and eT_R cells when DC abundance was dramatically increased following implantation of Flt3L-secreting B16 melanoma cells. Surprisingly, we found that increasing the number of DCs significantly expanded the eT_R cell population but did not impact cT_R cell abundance (Fig. 5.1). Moreover, DC-expanded Treg cells showed decreased Stat5 phosphorylation, and the Treg cell number was increased to a similar extent even when B16.Flt3L recipients were treated with α-IL-2 throughout the period of tumor growth (Fig. 5.2). Thus, rather than acting in the same pathway, these data strongly indicate that DCs and IL-2 act in parallel to control the abundance of distinct Treg cell subsets.

The co-stimulatory receptor ICOS helps to control regulatory T cell abundance and function *in vivo* (Burmeister *et al.*, 2008; Herman *et al.*, 2004), and ICOSL is highly expressed by DCs. Moreover, ICOS expression was dramatically upregulated in Treg cells from B16.Flt3L recipient mice (Fig. 5.3A), and we therefore evaluated the role of ICOS signaling in the homeostatic maintenance of eT_R cells in non-tumor-bearing mice using a blocking α-ICOSL antibody. Indeed, blockade of ICOS signaling for 2 weeks resulted in the specific loss of eT_R cells in both lymphoid and non-lymphoid tissues without any effect on cT_R cell abundance (Fig. 5.3B, C). This was not simply due to antibody-mediated depletion of these cells, as Treg cells do not express

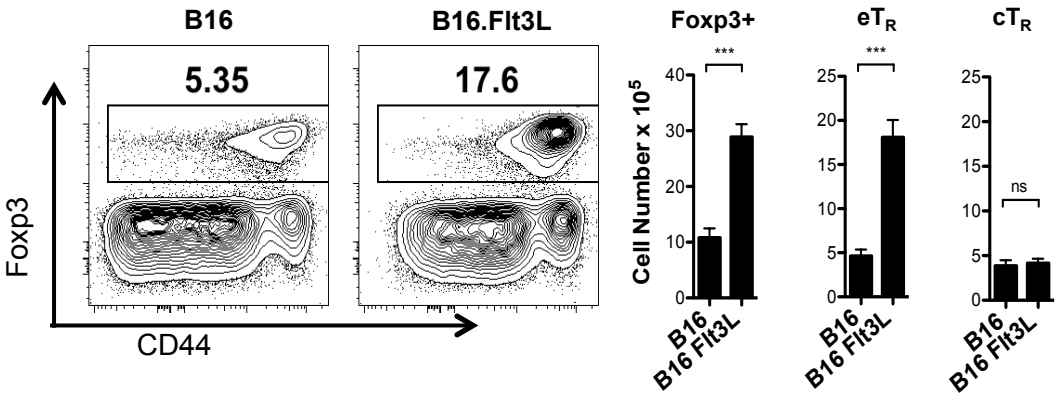

Figure 5.1. DC expansion-mediated Treg expansion selectively expands eT_R cells.
WT mice were injected subcutaneously with control B16 or Flt3L-expressing B16 (B16.Flt3L) tumor cells 2 weeks prior to analysis. After tumor formation, spleens were isolated, and CD4+ cells were analyzed for the expression of Foxp3, CD44, and CD62L by flow cytometry. The representative dot plots on the left show the frequencies of total $Foxp3^+$ cells, and the bar charts show the numbers of $Foxp3^+$, eT_R, and cT_R cells in animals given control B16 or B16.Flt3L tumor cells (n=3 mice per group).

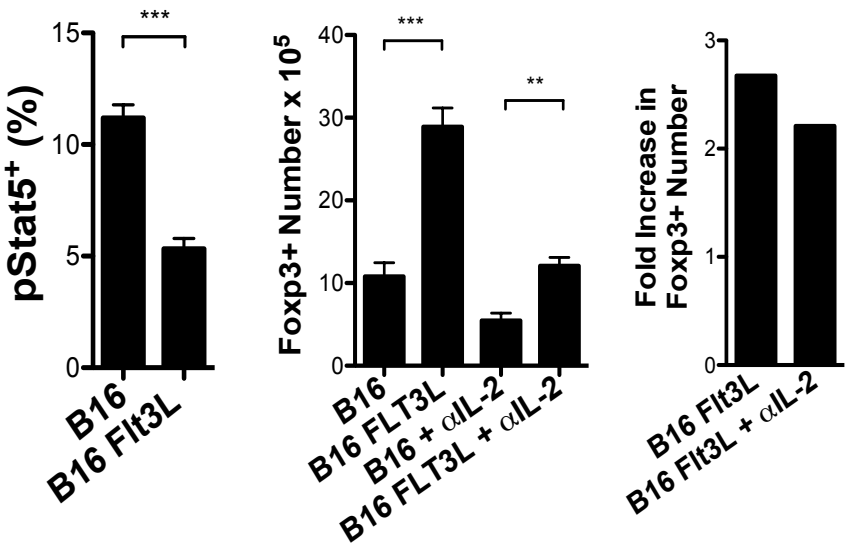

Figure 5.2. DC expansion-mediated Treg expansion occurs independent of IL-2 signaling.
(Left) The frequency of Stat5 phosphorylation among splenic Treg cells was evaluated by flow cytometry in mice given B16 or B16.Flt3L tumor cells (n=3 mice per group). (Right) Mice were injected subcutaneously with control B16 or B16.Flt3L tumor cells 2 weeks prior to analysis (n=6 per group). In addition, 3 mice in each group received intraperitoneal αIL-2 injections every 3 days during the period of tumor development. The number of splenic Treg cells (middle) and the average fold-increase in splenic Treg cell abundance (right) in mice given B16 or B16.Flt3L cells and/or treated with αIL-2 antibodies are shown.

significant amounts of ICOSL, and ICOSL-expressing B cells and DCs were present in normal numbers/frequencies in treated mice (data not shown). Mechanistically, αICOSL treatment did not reduce Stat5 phosphorylation in Treg cells (Fig. 5.3D), and thus the observed loss of eT_R cells in treated mice was not secondary to decreased IL-2 production. Surprisingly, despite its well-established co-stimulatory function, the remaining eT_R cells in αICOSL treated mice demonstrated normal expression of Ki-67 (Fig. 5.3D). However, ICOSL blockade led to selective loss of Bcl-2^{lo} Treg cells (Fig. 5.4), indicating that rather than inducing eT_R activation and proliferation, ICOS provides important anti-apoptotic signals that promote the survival of $Bcl2^{lo}Mcl1^{lo}$ eT_R cells.

TCR and inflammatory signals control the balance of cT_R and eT_R cells

The TCR repertoire of Treg cells is believed to be heavily biased toward autoreactivity, and as such, these cells are believed to undergo continual contact with self-antigen *in vivo* (Hsieh *et al.*, 2004; Moran *et al.*, 2011). However, the differential expression of activation markers by cT_R and eT_R cells suggests that they may differ in their extent of self-reactivity and degree of TCR stimulation, which could underlie their distinct homeostatic behaviors. To directly assess TCR signaling in cT_R and eT_R cells, we analyzed reporter mice expressing GFP from the *Nr4a1* (Nur77) locus, which is activated independent of co-stimulation upon TCR triggering (Moran *et al.*, 2011). Surprisingly, we observed only small differences in GFP expression between cT_R and eT_R cells, and both Treg cell populations demonstrated significantly increased expression in comparison to $CD4^+CD44^{lo}Foxp3^-$ naïve T cells (Fig. 5.5). Thus, differences in the extent of TCR triggering are unlikely to account for the distinct phenotypic and homeostatic properties of cT_R and eT_R cells.

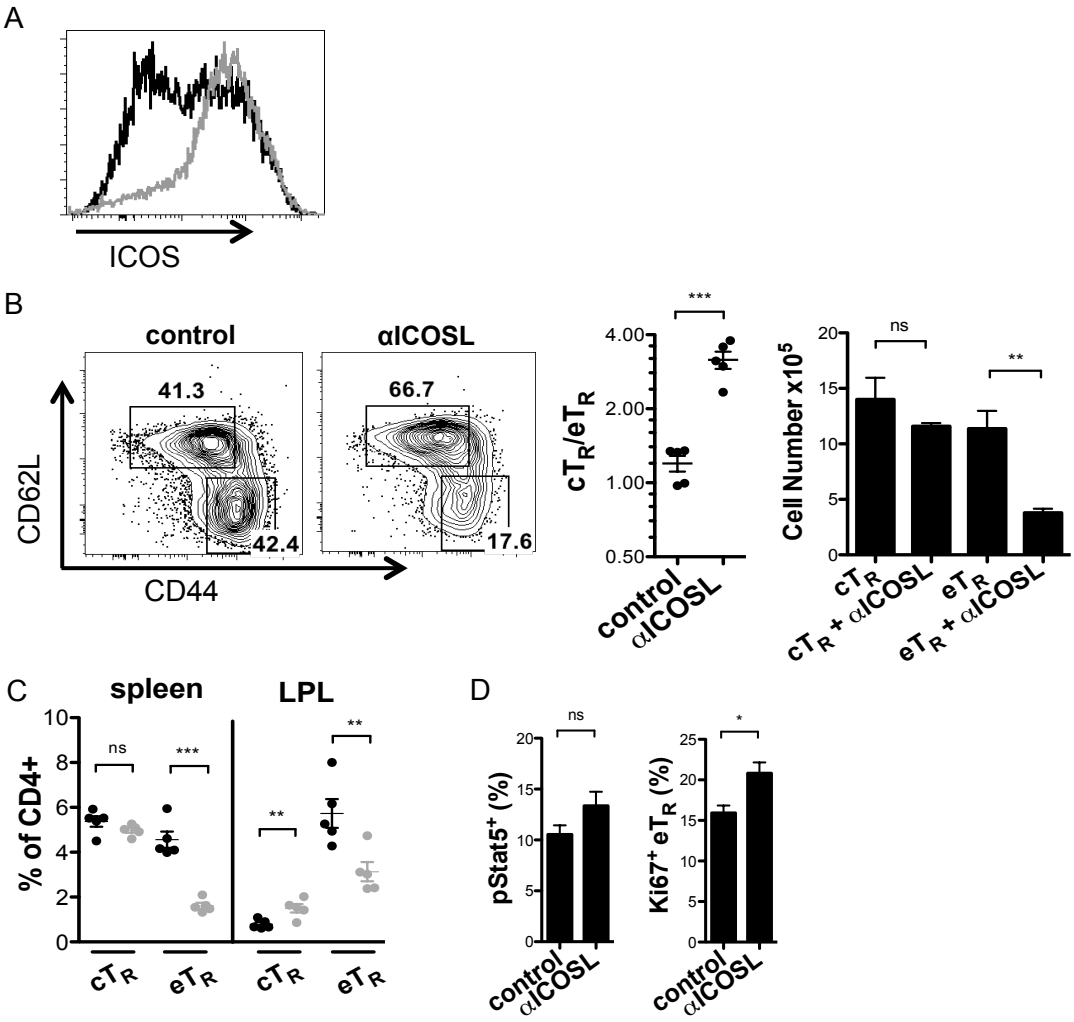

Figure 5.3. ICOS expression is required for the maintenance of eT_R cells.

(A) In mice injected with B16 (black) or B16.Flt3L (grey) tumor cells, the spleens were evaluated by flow cytometry after 2 weeks for the expression of Foxp3 and ICOS, as shown in a representative overlapping histogram. (B-D) WT mice were injected intraperitoneally with control or αICOSL antibody every 3 days for a period of 2 weeks. Lymphocytes from the spleen and lamina propria (LPL) were isolated and counted, and CD4+ cells were examined by flow cytometry for the expression of Foxp3, CD44, CD62L, pStat5, Ki-67, and Bcl-2. (B) In the spleen, representative cT_R and eT_R cell frequencies (left), the cT_R to eT_R cell ratio (middle), and cT_R and eT_R cell numbers (right) in control and α-ICOSL-treated mice are shown (n=5 mice per group). (C) The frequencies of cT_R and eT_R cells among $CD4^+$ cells in the indicated tissue sites following 2-week treatment with control (black circles) or α-ICOSL antibodies (grey circles) are shown (n=5 per group). (D) Stat5 phosphorylation and Ki-67 expression were evaluated by flow cytometry for total splenic Treg cells in 2-week control- and αICOSL-treated mice (n=5 per group).

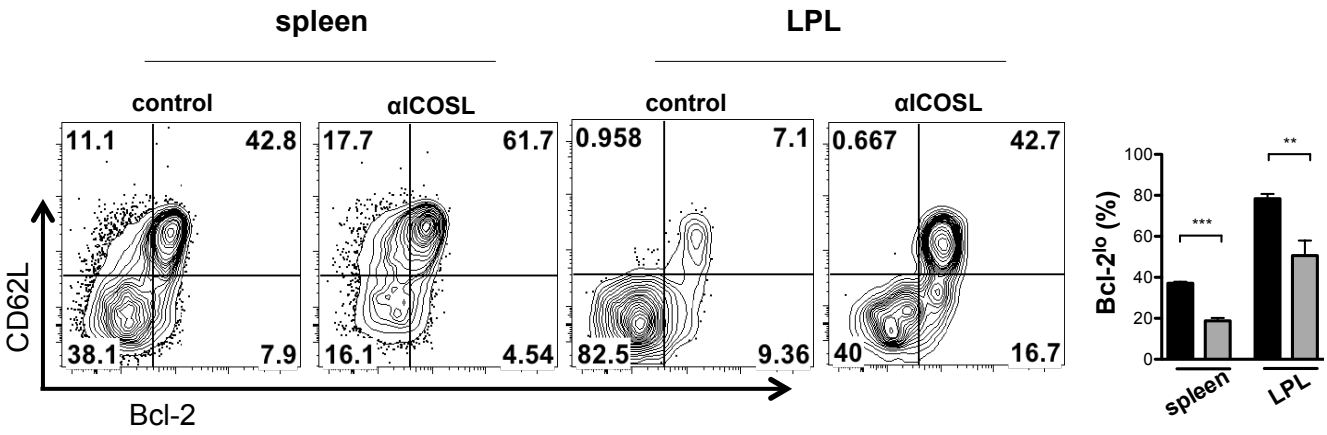

Figure 5.4. ICOS expression promotes the survival of eT_R cells.
Analysis of CD62L and Bcl-2 expression by Treg cells in the spleen and LPL from mice treated with control IgG (black bars) or α-ICOSL antibody (grey bars) for 2 weeks (n=5 per group).

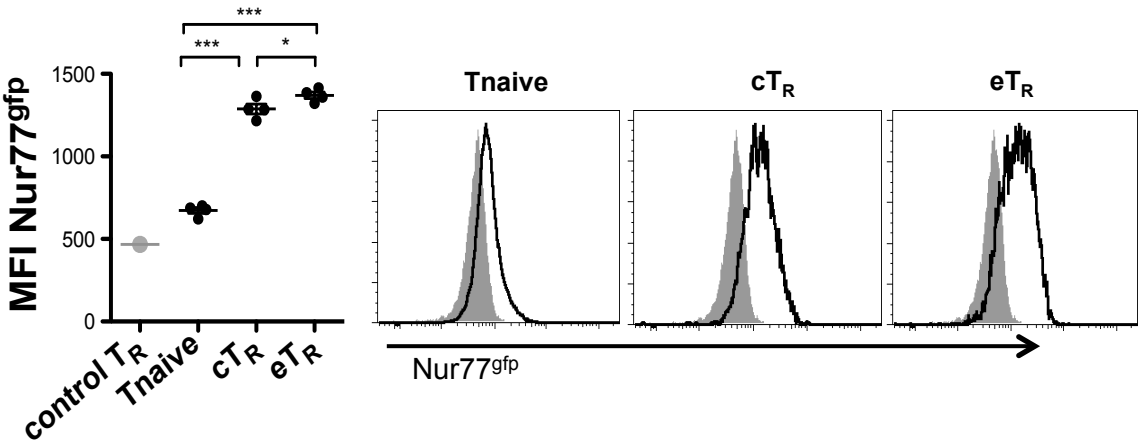

Figure 5.5. cT_R and eT_R differences are not due to different levels of basal TCR signaling.
Spleens from Nur77^{gfp} mice were obtained, and CD4+ cells were analyzed by flow cytometry for the expression of Foxp3, CD44, CD62L, and Nur77. The chart on the left shows the MFI for Nur77^{gfp} in WT splenic Treg cells (n=1 mouse) and CD4$^+$Foxp3$^-$CD44^{lo} naïve T cells, cT_R, and eT_R cells from Nur77^{gfp} mice (n=4 mice). The histograms at the right show representative Nur77^{gfp} expression in the indicated T cell populations, with the shaded histograms representing background fluorescence in total CD4+ T cells from a non-transgenic WT mouse.

To determine whether the inflammatory context of antigen recognition controls the expression of key molecules involved in cT_R and eT_R homeostasis, we studied OVA-specific Treg cells from DO11.10xRIP-mOVA (DORmO) mice (Walker *et al.*, 2003). In these RAG-sufficient mice, a large number of OVA-specific Treg cells develop in the thymus due to recognition of OVA as a self-antigen, and these cells can be identified based on their high-level expression of the KJ1-26 clonotypic TCR and distinguished from KJ1-$26^{lo/-}$ Treg cells that express endogenously rearranged TCRs. Interestingly, the KJ1-26^{hi} Treg cells are predominantly cT_R cells, whereas the bulk of eT_R cells are KJ1-$26^{lo/-}$ (Fig. 5.6). Thus, although both cT_R and eT_R cells appear to be largely self-reactive, T cell specificity appears to strongly influence the cT_R/eT_R phenotype. To further determine how antigen recognition influences eT_R differentiation, we transferred OVA-specific cT_R cells from DORmO mice into recipient mice systemically expressing soluble OVA under control of the metallothionein promoter (sOVA mice). Despite the high level of systemic self-antigen present, most transferred Treg cells did not proliferate, remained $CCR7^+$, and upregulated only low surface expression of ICOS in sOVA mice (Fig. 5.7). However, the addition of LPS as an inflammatory trigger greatly augmented Treg cell proliferation and induced a dramatic shift toward the $CCR7^{lo}ICOS^{hi}$ eT_R phenotype that was associated with loss of Stat5 phosphorylation (Fig. 5.7 and 5.8A). Similar results were observed when complete Freund's adjuvant was administered subcutaneously as an inflammatory stimulus (not shown). Finally, to examine the potential for polyclonal eT_R cells to access IL-2 in the context of inflammation, we assessed IL-2 signaling and Stat5 phosphorylation in endogenous cT_R and eT_R cells from LPS-treated mice and observed a slight decrease in Stat5 phosphorylation in cT_R cells but no change in the low level of Stat5 phosphorylation observed in eT_R cells (Fig. 5.8B). Thus, although both cT_R and eT_R cells are subject to continual TCR stimulation, inflammatory signals

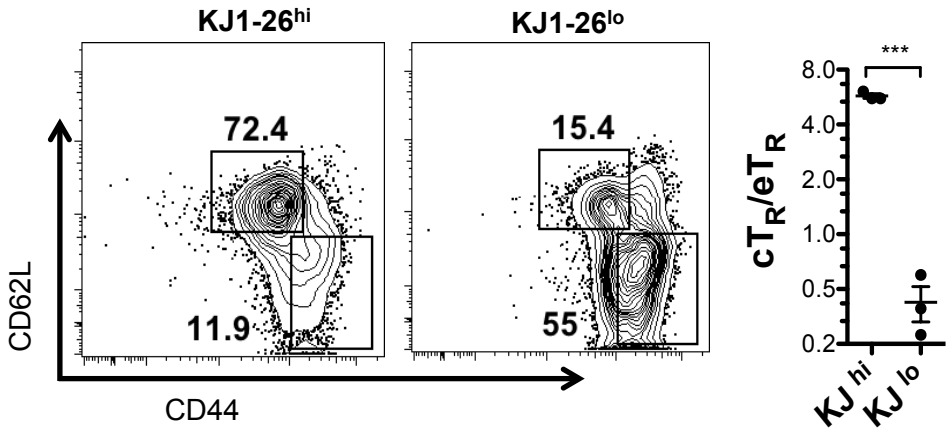

Figure 5.6. Influence of T cell specificity on the cT_R/eT_R phenotype. Spleens from unmanipulated DORmO mice were isolated, and CD4+ cells were examined by flow cytometry for Foxp3, DO11.10 TCR (KJ126), CD44, and CD62L expression. The plots show representative splenic cT_R and eT_R cell frequencies within the indicated Treg cell populations, and the chart quantifies the average cT_R to eT_R cell ratio in each group across 3 animals.

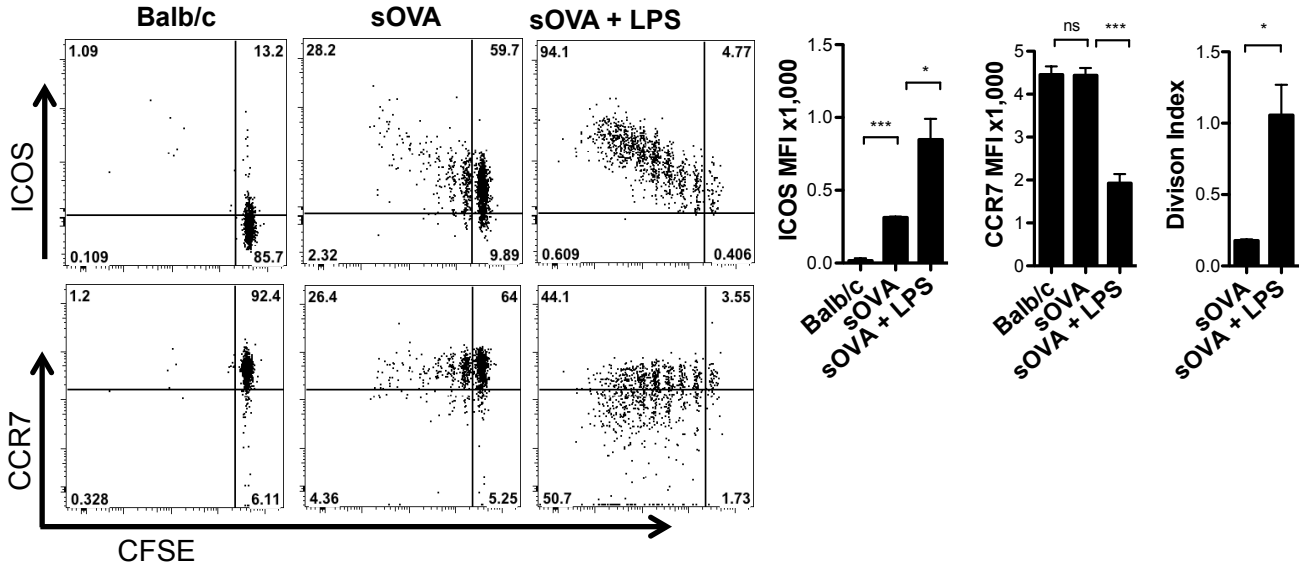

Figure 5.7. Antigen in the context of inflammation promotes the eT_R phenotype.
CD4+CD25+ cells ($1x10^6$) isolated from DORmO mice were CFSE labeled and adoptively transferred into Balb/c (n=3) or sOVA (n=6) mice; at the time of transfer, 3 of the mice in the sOVA group received intravenous injections of LPS. Six days after transfer, spleens were harvested, and CD4+KJ126+ cells were examined by flow cytometry for the expression of CD44, CD62L, ICOS, CCR7 and CFSE. CCR7 staining was performed using a CCL19-human IgGFc fusion protein. The FACS plots show representative staining for ICOS (top, left) and CCR7 (bottom, left) vs. CFSE in gated OVA-specific ($KJ126^+$) Treg cells after transfer into the indicated recipients. The MFI values for ICOS and CCR7 expression (middle) and the division index values based on CFSE dilution (right) for transferred $KJ126^+$ cells harvested from the indicated recipients are plotted at the right (n=3 mice per group).

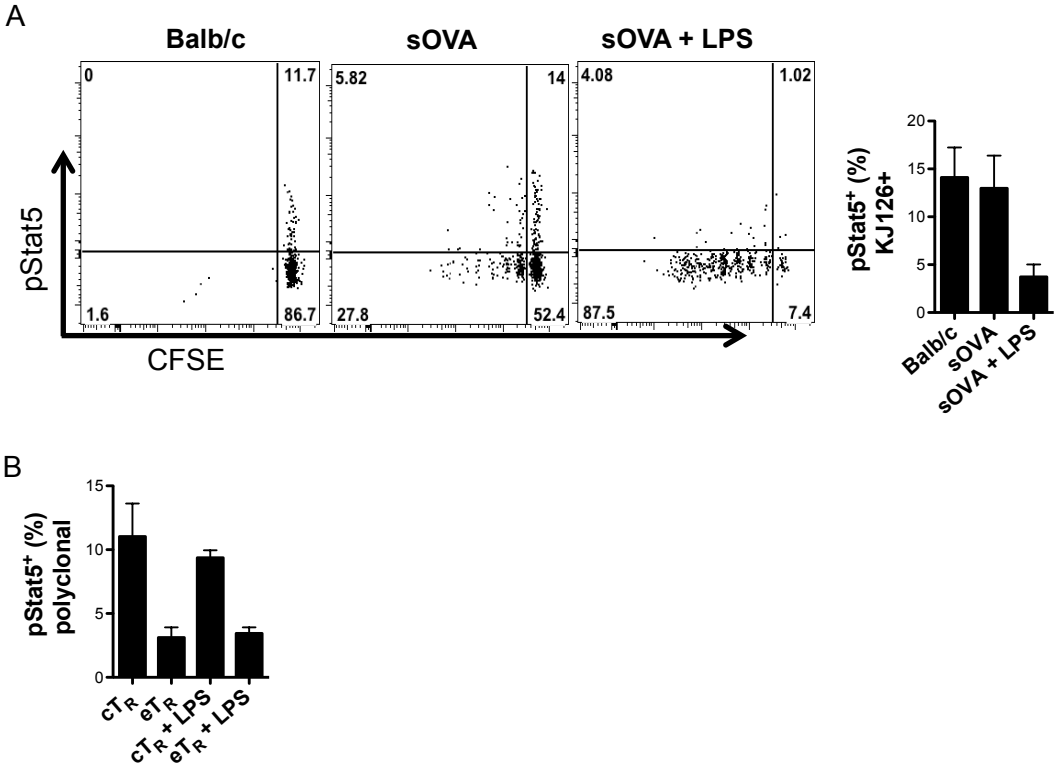

Figure 5.8. Antigen in the context of inflammation does not promote IL-2 signaling.
CD4+CD25+ cells ($1x10^6$) isolated from DORmO mice were CFSE labeled and adoptively transferred into Balb/c (n=3) or sOVA (n=6) mice; at the time of transfer, 3 of the mice in the sOVA group received intravenous injections of LPS. Six days after transfer, spleens were harvested, and CD4+KJ126+ cells were examined by flow cytometry. (A) The FACS plots show representative Stat5 phosphorylation vs. CFSE in OVA-specific $KJ126^+$ Treg cells after transfer into the indicated recipients. The percentage of transferred KJ126+ cells expressing pStat5 upon recovery is shown in the bar graph (n=3 mice per group). (B) The frequency of Stat5 phosphorylation was also evaluated by flow cytometry in endogenous, polyclonal cT_R and eT_R cells from control and LPS-treated sOVA recipient mice (n=3 mice per group).

in the immune environment alter Treg cell expression of key surface proteins that control their homeostatic requirements.

Examination of KLRG1-mediated negative Treg regulation

The above findings indicated that eT_R cells increase in frequency following strong activating or inflammatory stimuli. However, this transient eT_R cell increase is followed by a period of contraction to restore the homeostatic balance, which indicates that negative regulatory mechanisms function to curtail eT_R activation, expansion, or survival. Because ITIM-containing receptors such as KLRG1 are known to antagonize T cell activation and KLRG1 is highly expressed by eT_R phenotype cells, we examined the potential role for KLRG1 in the negative regulation of this activated Treg cell population.

Our data show that $KLRG1^+$ Treg are significantly enriched in peripheral tissues such as the skin and gut, and KLRG1 expression is consistently associated with high expression of the activation molecules CD44, ICOS, and CTLA-4, as well as the peripheral tissue homing molecules CD103, CCR4, and P-selectin ligand (Fig. 5.9 and data not shown). Because the KLRG1 ligand E-cadherin is expressed at high levels in barrier tissues such as the skin and the gut, we hypothesized that KLRG1 expression may result in location-specific inhibition of activated Treg cells. In line with this hypothesis, KLRG1 expression by Treg cells correlated with greater proliferation in lymphoid tissues yet reduced proliferation in non-lymphoid tissues, such as the skin and gut (Fig. 5.10).

To evaluate the functional significance of KLRG1 expression, we obtained *Klrg1*$^{-/-}$ mice from Dr. Hans-Peter Pircher at the Department of Immunology, University of Freiburg, Germany. Because no apparent defects were observed in any T cell subset in *Klrg1*$^{-/-}$ animals, we chose to evaluate the cell-intrinsic function of KLRG1 when knockout (KO) cells were placed in competition with WT cells in the 50/50 mixed

bone marrow chimera (BMC) setting. Because these BMC mice contain large numbers of normal WT bone marrow-derived cells (in addition to a normal non-hematopoietic cell compartment), any potential deficit in KO cell expansion and maintenance can be measured according to the ratio of WT:KO cells recovered after 8-10 weeks of hematopoietic reconstitution following lethal irradiation and bone marrow transfer. As shown in Fig. 5.12, the input frequency of WT (CD45.1+) and KLRG1-deficient (CD45.2+) bone marrow was approximately 50/50, and the recovery of Gr-1+ neutrophils from the spleen was approximately 50/50 as well (Fig. 5.11). However, upon comparison of control WT/WT BMCs (n=5) and KLRG1KO/WT BMCs (n=9), we consistently observed a skewing in the WT:KO Treg cell ratio in favor of KO cells, but only in peripheral tissues such as the gut and skin (Fig. 5.12 B). Furthermore, in this mixed BMC setting, we found that $CD44^{hi}$ Treg cells also demonstrated skewing towards the KO lineage, and this effect was significant for all tissues examined (Fig. 5.12). These results suggested that KLRG1-deficient Treg cells were more efficient at achieving an activated state and populating peripheral tissues due to their inability to receive signals through a negative regulatory molecule.

Finally, to evaluate whether KLRG1-deficient Treg cells would respond differently to inflammation compared to WT cells, specifically with the hypothesis that KO cells would expand or proliferate to a greater extent, we employed multiple models of localized tissue inflammation or systemic infection. First, using the $CD45RB^{hi}$ model of adoptive T cell-mediated colitis, we found that equal proportions of WT and KLRG1-deficient Treg cells transferred prior to disease onset (prevention model) or during active disease (treatment model) demonstrated a similar activation profile, proliferation status, and cell number recovered from the inflamed colon at the time of sacrifice (data not shown). In addition, mixed BMC mice were infected with *Listeria monocytogenes* expressing ovalbumin (LmOVA), and at days 3 and 7 after

infection, these mice demonstrated equal proportions of WT- and KO-derived Treg cells (as well as CD8+ effector/memory cells) with a similar activation profile (data not shown). To address the responses of KLRG1-deficient Treg cells in the skin, mixed BMC mice were subjected to 2,4-dinitrofluorobenzene (DNFB)-mediated contact hypersensitivity (CHS) responses in the skin. Following 2 applications of DNFB to the ear for sensitization (days 0 and 1) and then a repeated application on day 6 for challenge, mice were sacrificed 48 hours after challenge, and the ratio of WT:KO Treg cells and their proliferation was evaluated for cells recovered from the affected and non-affected contralateral control tissue. Although the previously observed increased frequency of KLRG1 KO-derived cells was confirmed in the ear, the inflammatory response associated with CHS did not further skew this ratio or significantly affect the increased proliferation of cells at the site of inflammation (Fig. 5.13). Thus, although KLRG1-deficient cells consistently showed an improved ability to reconstitute the mixed BMC environment in peripheral tissues, this finding could not be further manipulated as a result of inflammation or explained in the context of improved proliferation or persistence post transfer.

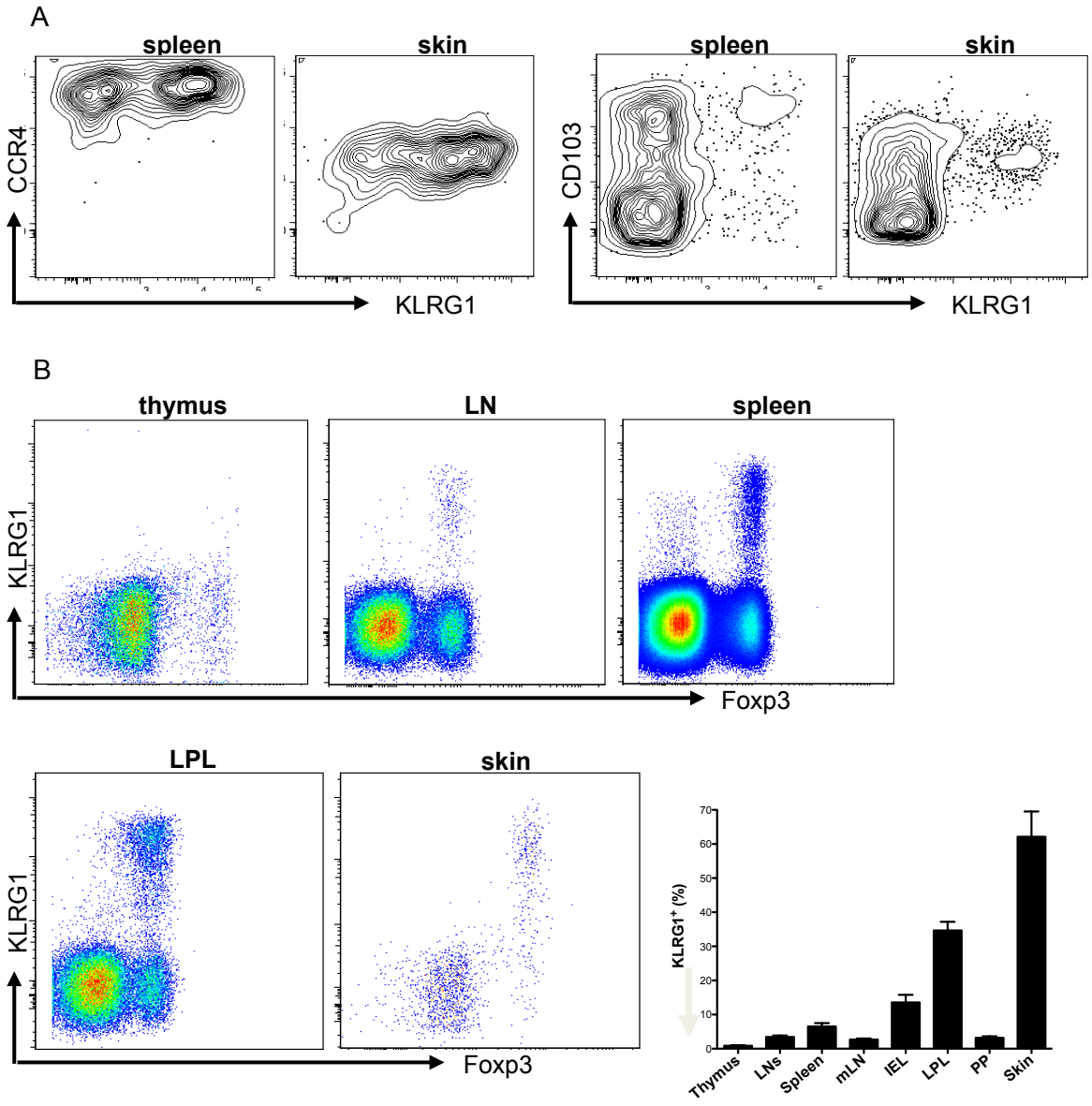

Figure 5.9. KLRG1 expression is associated with peripheral tissue homing.
Cells from WT mice were harvested from the indicated tissues and examined by flow cytometry for expression of Foxp3, CD44, KLRG1, CCR4, and CD103. A) Representative FACS plots gated on Foxp3+ cells showing KLRG1 expression in relation to CCR4 and CD103 expression. B) KLRG1 expression by Foxp3+ cells was examined in a variety of tissues, and the frequency of KLRG1+ cells among total Foxp3+ cells is plotted in the bar graph.

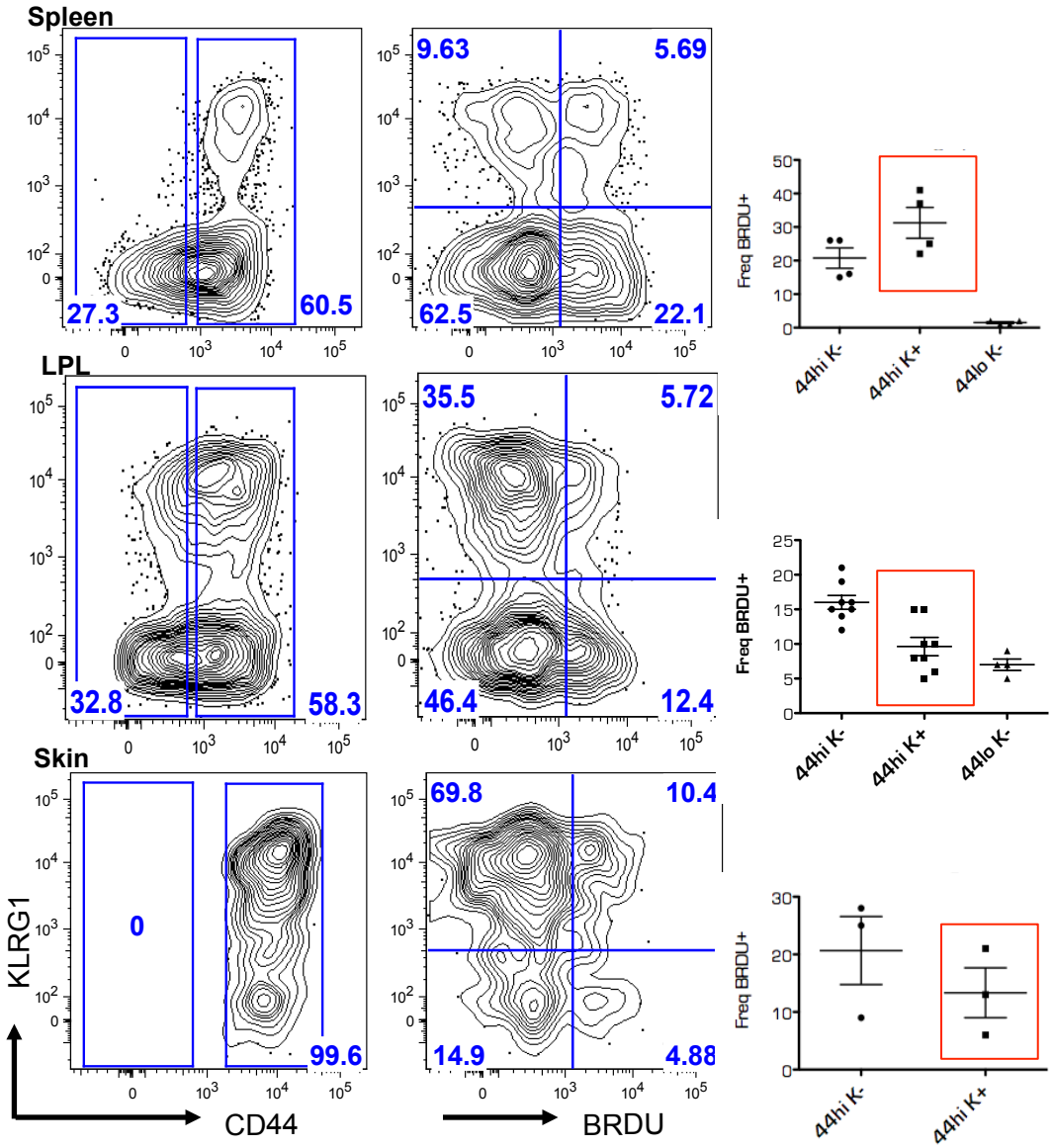

Figure 5.10. KLRG1^{+} Treg cells show reduced proliferation in peripheral tissues.
WT mice were administered BRDU in their drinking water for 3 days prior to analysis. Cells from the indicated tissues were harvested, and CD4+ cells were examined by flow cytometry for expression of Foxp3, CD44 and KLRG1 and BRDU incorporation. The representative FACS plots on the left are gated on Foxp3+ cells and show KLRG1 expression in relation to CD44 expression and BRDU incorporation. The frequency of BRDU+ cells among CD44^{hi}KLRG1- cells, CD44^{hi}KLRG1+ cells and CD44^{lo}KLRG1- cells is shown at the right (n=3-8 measurements per population).

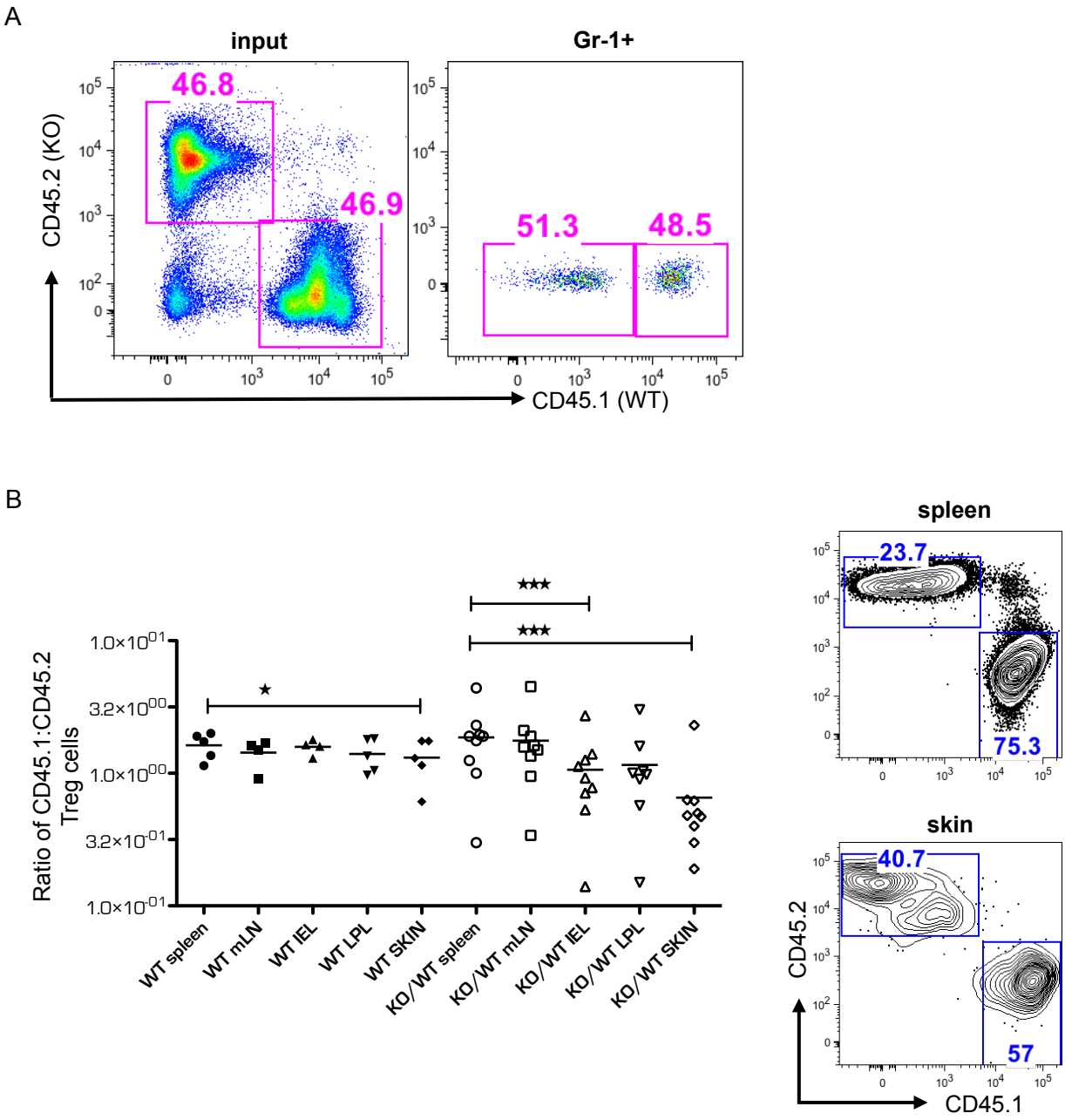

Figure 5.11. In mixed bone marrow chimeras, KLRG1-deficient Treg cells are more abundant in peripheral tissues.
Mixed BMCs were created by injecting a 50/50 mix of WT (CD45.1) and KLRG1-deficient (CD45.2) bone marrow cells into TCRβδ KO mice. Control chimeras were also made with CD45.1 WT and CD45.2 WT bone marrow. After 8 weeks of reconstitution, cells from the indicated tissues were harvested, and CD4+ cells were examined by flow cytometry for expression of Foxp3, CD45.1 and CD45.2. A) As a control for equal loading and reconstitution of cells, input cells and Gr-1+ cells (which were not found to express KLRG1 at any time during reconstitution) were evaluated for WT/KO origin. B) CD4+ Foxp3+ cells were examined in the indicated tissues, obtained from WT control chimeras (left of graph) and KO/WT mixed chimeras (right of graph), for the ratio of CD45.1+ cells to CD45.2+ cells. Representative FACS staining from the spleen and skin for KO/WT chimeras is shown at the far right.

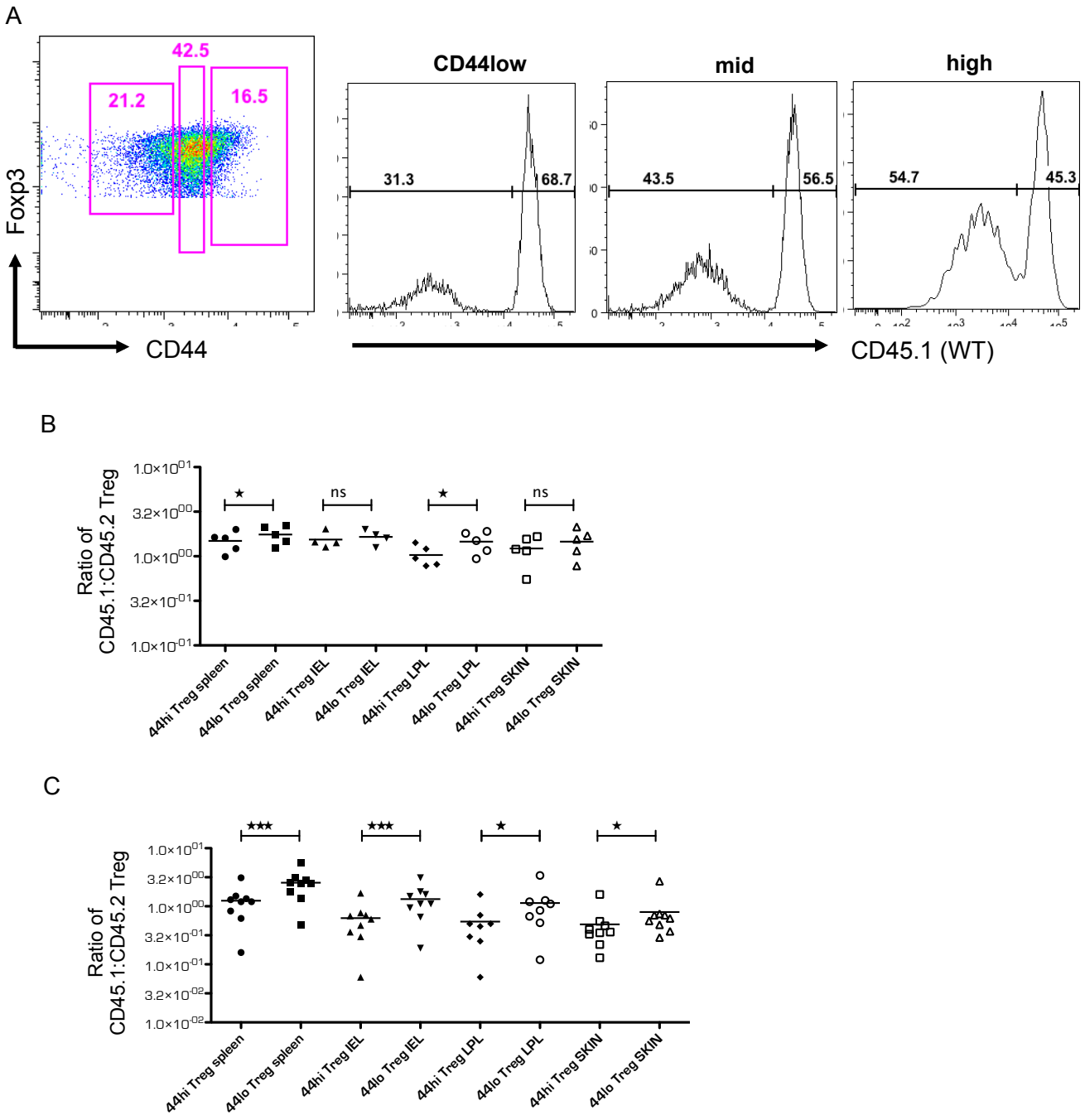

Figure 5.12. CD44^{hi} Treg cells show enhanced skewing towards KLRG1-deficient bone marrow progenitors.
After 8 weeks of reconstitution, Treg cells from the spleen were examined by flow cytometry for expression of Foxp3, CD44, CD45.1 and CD45.2. A) Foxp3+ cells were gated according to CD44 expression level, and the representative proportions of CD45.1+ WT-derived cells are shown for each population. B) Foxp3+ cells from WT control chimeras were examined in the indicated tissues for the ratio of WT/KO cells based on high or low expression of CD44. C) Foxp3+ cells from KO/WT chimeras were examined as in B.

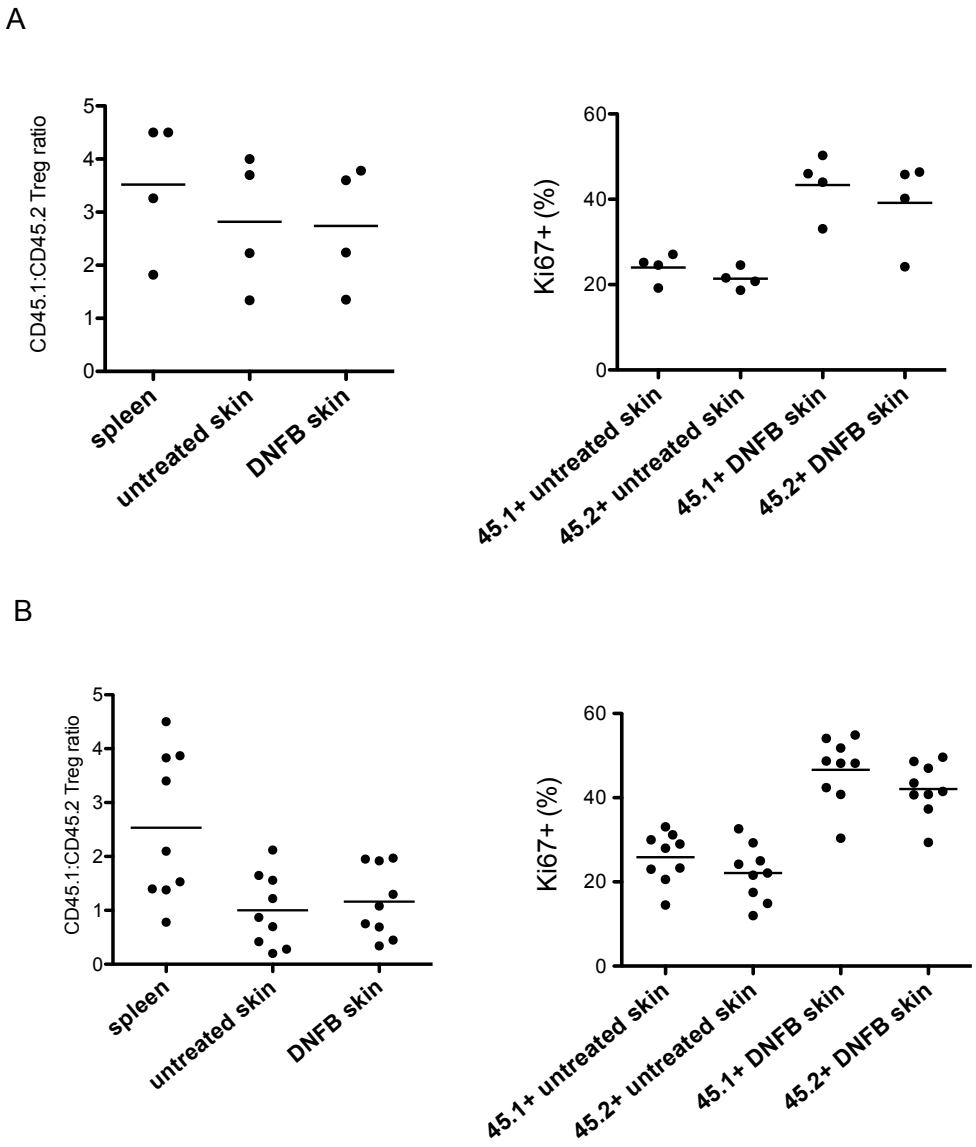

Figure 5.13. The frequencies of KLRG1-deficient Treg cells are not altered in response to skin inflammation.
Forty-eight hours after DNFB challenge, WT control (A) and KO/WT mixed chimeras (B) were sacrificed, and Foxp3+ cells from the spleen and skin were evaluated for the ratio of CD45.1:CD45.2+ cells (left graphs). In the skin, Total Foxp3+ cells were then evaluated for Ki-67 expression, and frequency of Ki-67+ Treg cells (right graphs) was evaluated for each CD45 cell population form treated or untreated skin. 'Untreated skin' represents the contralateral control ears from challenged mice.

CHAPTER 6: Discussion

Despite extensive scrutiny, the mechanisms controlling Treg cell abundance and function *in vivo* remain poorly defined. Our findings provide an integrated understanding of how IL-2 and antigen receptor/co-stimulatory signals control the maintenance of homeostatically distinct Treg cell populations in different anatomical locations. Taken together, our data support a model in which re-circulating $CCR7^+$ cT_R cells are sustained by paracrine IL-2 signaling from other T cell populations within secondary lymphoid tissues. When activated in the presence of inflammatory signals, quiescent cT_R cells differentiate into rapidly proliferating eT_R cells, lose CCR7 expression, and redistribute to non-lymphoid environments. Having lost access to IL-2, eT_R cells are highly prone to apoptosis and must rely on alternative signals such as continued ICOS signaling for their homeostatic maintenance. Thus, cT_R and eT_R cells are maintained as separate pools of cells with distinct homeostatic requirements, and this represents a fundamental subdivision among Treg cells.

The role of IL-2 in the development, maintenance, and function of Treg cells is complex (Malek *et al.*, 2008). The constitutive expression of the high-affinity IL-2 receptor by Treg cells and the colitis and inflammatory disease that develop in mice lacking IL-2 or CD25 strongly indicate that IL-2 is critical for Treg cell-dependent immune tolerance. However, IL-2 and the related cytokine IL-15 are partially redundant in the thymic development of Treg cells, and thus *Il2*$^{-/-}$ and *Il2ra*$^{-/-}$ mice contain normal numbers of peripheral Treg cells (Burchill *et al.*, 2007; Fontenot *et al.*, 2005; Soper *et al.*, 2007). Moreover, boosting Treg cell numbers in *Il2*$^{-/-}$ mice via deletion of the pro-apoptotic protein Bim failed to prevent autoimmune disease development (Barron *et al.*, 2010), indicating that despite its ability to induce Treg cell proliferation and survival, the principle effect of IL-2 on Treg cell function is

qualitative rather than quantitative. Current hypotheses to explain how Treg cells in these mice fail to control the development of autoimmunity include impaired metabolic fitness of Treg cells (Fontenot *et al.*, 2005), reduced Foxp3 expression (Burchill *et al.*, 2007), and the failure to obtain a 'mature', or $CD25^{hi}$, pool of peripheral Treg cells (Cheng *et al.*, 2011). However, our results demonstrate that rather than acting as a global survival or maturation factor, IL-2 predominantly controls the homeostatic maintenance of a specific Treg subset, which supports the notion that maintaining immune tolerance requires the coordinated action of both cT_R and eT_R cells. Indeed, multiple mechanisms of immune suppression are used by Treg cells (Vignali *et al.*, 2008), and at least some of these mechanisms segregate in cT_R and eT_R phenotype cells. For instance, whereas cT_R cells are ideally positioned to interact with and inhibit the function of antigen-presenting cells in secondary lymphoid tissues and thereby prevent the priming of autoreactive T cells (Tadokoro *et al.*, 2006), the production of IL-10 in non-lymphoid tissues is restricted to the eT_R population and is driven in large part by their selective expression of the transcription factor Blimp-1 (Cretney *et al.*, 2011; Cretney *et al.*, 2013).

The loss of cT_R cells in the absence of IL-2 signaling is likely due to a combination of factors. As a quiescent, transitory population, the abundance of cT_R cells is a function of their generation in the thymus, their survival, and their conversion into eT_R phenotype cells during inflammation. Interestingly, a recent study demonstrated that IL-2 can directly boost expression of the anti-apoptotic protein Mcl1 and thereby enhance Treg cell survival (Pierson *et al.*, 2013), and we confirmed that cT_R cells express higher levels of Mcl1 than eT_R cells. Thus, impaired cT_R survival in the absence of IL-2 signaling may lead to the initiation of dysregulated inflammatory responses, which may further contribute to cT_R loss by promoting cT_R conversion to eT_R cells. This would eventually lead to the near complete depletion of cT_R cells and

massive expansion of activated $CD4^+$ and $CD8^+$ T cells observed in *Il2*$^{-/-}$ and *Il2ra*$^{-/-}$ mice, which would eventually overwhelm the remaining eT_R cells and cause peripheral autoimmunity. Indeed, indicative of a selective loss of cT_R activity in secondary lymphoid tissues, one of the most striking phenotypes in CD25-deficient mice is the rapid development of lymphadenopathy and splenomegaly, which is associated with an accumulation of activated $CD4^+$ and $CD8^+$ T cells and precedes the development of peripheral autoimmunity (Willerford *et al.*, 1995).

Whereas IL-2 can induce Treg cell proliferation when present in excess after administration of super-agonistic IL-2/αIL-2 immune complexes or during 'niche-filling' after acute Treg cell depletion (Boyman *et al.*, 2006; Pierson *et al.*, 2013), we found that IL-2 signaling is not associated with Treg cell proliferation in the steady state. Indeed, using several experimental systems, we demonstrated that the rapid proliferation of eT_R cells is IL-2-independent. However, although not required for their homeostatic maintenance/proliferation, eT_R cells remain highly responsive to IL-2 *in vitro* and *in vivo*, and we cannot rule out the possibility that IL-2 signaling does helps regulate the function of eT_R cells. For instance, sequestration of IL-2 by Treg cells has been shown to limit the responses of both T and NK cells (Pandiyan *et al.*, 2007; Gasteiger *et al.*, 2013; Sitrin *et al.*, 2013). Nonetheless, the presence of functionally intact eT_R cells in IL-2- and CD25-deficient mice is consistent with the substantially delayed development of autoinflammatory disease in these animals relative to that observed in Foxp3-deficient *scurfy* mice or *Il2rb*$^{-/-}$ mice that lack essentially all Treg cells (Godfrey *et al.*, 1991; Soper *et al.*, 2007).

T cell migration and homeostasis are tightly linked, as cells need to access appropriate immune compartments endowed with important survival/proliferation factors (Sallusto and Mackay, 2004). However, although cT_R cells rely on paracrine IL-2, the microenvironmental IL-2 'niche' for Treg cells is poorly defined. Our results

demonstrate that this paracrine IL-2 signaling occurs almost exclusively within the organized T cell zones of secondary lymphoid tissues and requires expression of the chemokine receptor CCR7. The T cell zones of secondary lymphoid tissues are not homogenous, but instead can be further divided into a number of specialized domains that differ in cellular composition and function. This organization is largely dictated by non-hematopoietic stromal cells, which have recently been identified as key accessory cells that help promote immune function and tolerance (Malhotra *et al.*, 2013). Among their functions, stromal cells highly express the CCR7 ligands CCL19 and CCL21 (Luther *et al.*, 2000), raising the possibility that these cells act as cellular 'scaffolds' that bring $CCR7^+$ Treg cells into close proximity with other cells required for paracrine IL-2 signaling. Indeed, T cells rapidly migrate along the stromal cell network in a CCR7-dependent manner, and this promotes cellular and molecular interactions that support their activation and survival (Worbs *et al.*, 2007). For cT_R cells, migration along the stroma may bring them into proximity with $CCR7^+$ central memory cells, which can be potent source of IL-2 (Sallusto *et al.*, 1999), and $CCR7^+$ DCs, which could act as APCs to help trigger IL-2 production from conventional T cells. However, defining the function of specific stromal cell, T cell, and DC populations in facilitating paracrine IL-2 signaling to cT_R cells requires further investigation.

The multi-organ autoimmunity that develops in aged *Ccr7*$^{-/-}$ mice has been associated with deficits in the *in vivo* function of Treg cells resulting from improper selection in the thymus, as well as impaired migration in the periphery (Worbs *et al.*, 2007). However, similar to *IL2ra*$^{-/-}$ mice, *Ccr7*$^{-/-}$ mice have normal numbers of Treg cells with preserved *in vitro* suppressive activity (Schneider *et al.*, 2007). By demonstrating an intimate association between CCR7 expression by Treg cells and IL-2 signaling, our data help explain the activated, peripheral tissue phenotype of the

Treg cells in *Ccr7*$^{-/-}$ mice and also provide additional mechanistic insight into the link between CCR7, Treg cell function, and the development of autoimmunity. Interestingly, multiple polymorphisms in the *CCL21* gene have been associated with the development of rheumatoid arthritis in both European and Korean populations (Raychaudhuri *et al.*, 2008; Freudenberg *et al.*, 2011). Although the mechanisms driving this association are currently not understood, our data raise the intriguing possibility that defects in CCR7-dependent IL-2 signaling in Treg cells may contribute to development of human autoimmune disease.

eT_R cells are highly enriched in non-lymphoid tissues such as the intestines, and our parabiosis results demonstrate that these cells undergo minimal external replacement and thus must be maintained largely by balanced proliferation and cell death. However, unlike IL-2-dependent cT_R cells, we found that the maintenance of eT_R cells required continued ICOS-ICOSL engagement. ICOS is a potent co-stimulatory receptor that helps control the development and function of nearly all $CD4^+$ effector T cells subsets, including Th1, Th2, Th17, Tfh, and Treg cells (Simpson *et al.*, 2010). Indeed, consistent with its role in supporting eT_R cells, multiple studies have demonstrated that ICOS is essential for proper Treg cell function *in vivo* in a variety of inflammatory models (Burmeister *et al.*, 2008; Dong and Nurieva, 2003; Herman *et al.*, 2004; Ito *et al.*, 2008). Despite its co-stimulatory function, our data are most consistent with a role for ICOS in promoting eT_R survival rather than proliferation. Although the mechanisms by which ICOS promotes cell survival are poorly understood, they likely involve its ability to potently activate the pro-survival PI3K/Akt signaling pathway (Gigoux *et al.*, 2009).

Surprisingly, despite the preferential expression of activation markers such as CD69 by eT_R cells, we found that both cT_R and eT_R cells are subject to continued TCR stimulation *in vivo*. Thus, these results imply that it is the inflammatory context of

antigen recognition that controls the homeostatic switch between cT_R and eT_R cells. This is consistent with recently published work from our lab and others demonstrating that Treg cells alter their phenotypic and functional characteristics in response to various cytokine signals in the immune environment (Chaudhry *et al.*, 2011; Koch *et al.*, 2012; Hall *et al.*, 2012). LPS and other inflammatory stimuli potently upregulate expression of the co-stimulatory ligands CD80 and CD86 by DCs, and enhanced engagement of co-stimulatory receptors such as CD28 likely underlies the homeostatic changes that occur during eT_R differentiation. For instance, ICOS is upregulated downstream of NFATc2 and ERK activation following TCR/CD28 engagement (Tan *et al.*, 2006). Additionally, both CD28 and ICOS are potent activators of the PI3K/Akt signaling pathway, which, in addition to promoting cell survival, can trigger phosphorylation of the transcription factor Foxo1, leading to its sequestration in the cytoplasm and downregulation of Foxo1 target genes such as *Klf2* and *Ccr7* (Ouyang and Li, 2011). Importantly, continued TCR triggering distinguishes eT_R cells from recently characterized regulatory memory cells, whose maintenance in peripheral tissues is IL-7-dependent (Gratz *et al.*, 2013; Rosenblum *et al.*, 2011). Accordingly, we found that both the abundance and proliferation of eT_R cells are normal in IL-7-deficient mice (unpublished observations).

The study of negative regulatory receptors holds promise for therapies aiming to curtail Treg cell activity, in conditions such as cancer or chronic infection. We evaluated the potential for KLRG1 to serve as a negative regulator of Treg cell function, given its high steady-state level of expression on activated eT_R cells. Although we found that KLRG1 expression was associated with peripheral tissue homing and could be upregulated on Treg cells during periods of inflammation (similar to the recent study by Malek *et al.*, (2012)), we failed to identify the functional significance of this expression and were unable to demonstrate that KLRG1

ligation had any negative impact on Treg cell activation, proliferation, or function. However, negative T cell regulation is known to be the culmination of a variety of signals, and it is possible that the role of KLRG1 is redundant in the presence of other receptors such as PD-1 or CTLA-4. Also, although the structural and ligand-binding properties of human and mouse KLRG1 are very similar, KLRG1-mediated inhibition under physiological conditions was only shown to occur with human lymphocytes. In particular, murine KLRG1 exhibited a significantly lower inhibitory capacity compared to the human homolog due to its expression in the form of monomers, dimers, trimers, and tetramers, whereas functional signaling in the human form was the result of exclusive expression of the dimerized form (Hofmann *et al.*, 2012). Thus, the potential contribution of KLRG1 expression to the negative regulation of T cell responses in the mouse may be limited, and further work is required to evaluate why such significant populations of adaptive immune cells express this molecule in a defined, temporal pattern during the course of an immune response.

Manipulating Treg cell function and/or abundance represents an attractive therapeutic strategy to either boost or inhibit immune responses in a variety of clinical settings, and infusion of *ex vivo*-generated or expanded Treg cells is actively being pursued to treat autoimmunity and prevent allograft rejection (Riley *et al.*, 2009). However, competition for growth and survival factors acts to limit the size of the Treg cell pool *in vivo*, and, as a result, clinical trials of adoptive Treg cell therapy have failed to achieve long-term cell engraftment or substantial clinical benefit (Hippen *et al.*, 2011). A detailed understanding of the key factors that control the abundance and function of Treg cells in different tissue sites *in vivo* is therefore integral to the successful implementation of Treg cell-based cellular therapy. Our results defining distinct IL-2 and ICOS-dependent Treg cell populations in different

tissue environments have clear implications for the development of therapies aimed at boosting or inhibiting Treg cell activity in the context of autoimmune/inflammatory disease, transplantation, cancer and chronic infection (Jenabian *et al.*, 2012; Long *et al.*, 2013; Rech *et al.*, 2012; Tang *et al.*, 2012). Moreover, our findings help explain how polymorphisms in each of these pathways may contribute to Treg cell dysfunction during the development of autoimmunity (Raychaudhuri *et al.*, 2008; Takahashi *et al.*, 2009; Wang et al., 2009).

Concluding Remarks

In this study, we identify a fundamental subdivision in Treg cells associated with differential tissue localization and engagement of distinct homeostatic pathways. Instead of acting as a pan-Treg cell growth/survival factor, we found that IL-2 was uniquely required to maintain quiescent $CCR7^{hi}CD44^{lo}CD62L^{hi}$ Treg cells and that loss of IL-2 signaling was not associated with impaired Treg cell proliferation. Furthermore, we identified the chemokine receptor CCR7 as a key factor that provides these cells access to IL-2 in secondary lymphoid tissues. In contrast, although they remain IL-2 responsive, we found that $CD44^{hi}CD62L^{lo}CCR7^{lo}$ cells have reduced IL-2 signaling *in vivo*, and that the maintenance of these cells is IL-2-independent but relies on signals delivered by DCs and ICOS. Together, these data provide a new framework for understanding Treg cell homeostasis in different tissue sites that will be useful in developing and assessing strategies to therapeutically manipulate Treg cell function in a variety of immune-mediated diseases.

References

Au-Yeung BB et al. A genetically selective inhibitor demonstrates a function for the kinase Zap70 in regulatory T cells independent of its catalytic activity. Nat Immunol 2010; **11**(12):1085-92.

Bar-On L, Birnberg T, Kim KW, Jung S. Dendritic cell-restricted CD80/86 deficiency results in peripheral regulatory T-cell reduction but is not associated with lymphocyte hyperactivation. Eur J Immunol 2011; **41**(2):291-8.

Barron L, Dooms H, Hoyer KK, Kuswanto W, Hofmann J, O'Gorman WE, Abbas AK. Cutting edge: Mechanisms of IL-2-depedent maintenance of functional regulatory T cells. J Immunol 2010; **185**: 6426-30.

Beyersdorf N, Ding X, Tietze JK, Hanke T. Characterization of mouse CD4 T cell subsets defined by expression of KLRG1. Eur J Immunol 2007; **37**:3445-54.

Boursalian TE, Golob J, Soper DM, Cooper CJ, Fink PJ. Continued maturation of thymic emigrants in the periphery. Nat Immunol 2004; **5**:418-425.

Boyman O, Kovar M, Rubinstein MP, Surh CD, Sprent J. Selective stimulation of T cell subsets with antibody-cytokine immune complexes. Science 2006; **311**:1924-27.

Burchill MA, Yang J, Vogtenhuber C, Blazar BR, Farrar MA. IL-2 receptor beta-dependent STAT5 activation is required for the development of Foxp3+ regulatory T cells. J Immunol 2007; **178**(1):280-90.

Burmeister Y et al. ICOS controls the pool size of effector-memory and regulatory T cells. J Immunol 2008; **180**(2):774-82.

Burzyn D, Benoist C, Mathis D. Regulatory T cells in nonlymphoid tissues. Nat Immunol 2013; **14**(10):1007-13.

Chaudhry A, Rudra D, Treuting P, Samstein RM, Liang Y, Kas A, Rudensky AY. CD4+ regulatory T cells control Th17 responses in a Stat3-dependent manner. Science 2009; **326**(5955):986-91.

Cheng G, Yu A, Malek TR. T-cell tolerance and the multi-functional role of IL-2R signaling in T-regulatory cells. Immunol Rev 2011; **241**(1):63-76.

Cheng G, Yuan X, Tsai MS, Podack ER, Yu A, Malek TR. IL-2 receptor signaling is essential for the development of Klrg1+ terminally differentiated T regulatory cells. J Immunol 2012; **189**:1780-91.

Chung Y et al. Follicular regulatory T cells expressing Foxp3 and Bcl-6 suppress germinal center reactions. Nat Med 2011; **17**(8):983-8.

Cinamon G, Zachariah MA, Lam OM, Foss FW Jr, Cyster JG. Follicular shuttling of marginal zone B cells facilitates antigen transport. Nat Immunol 2008; **9**:54-62.

Cretney E et al. The transcription factors Blimp-1 and IRF4 jointly control the differentiation and function of effector regulatory T cells. Nat Immunol 2011; **12**(4):304-11.

Cretney E, Kaillies A, Nutt SL. Differentiation and function of Foxp3+ effector regulatory T cells. Trends Immunol 2013; **34**:74-80.

Darrasse-Jeze G et al. Feedback control of regulatory T cell homeostasis by dendritic cells in vivo. J Exp Med 2009; **206**(9):1853-62.

Delgoffe GM et al. The mTOR kinase differentially regulates effector and regulatory T cell lineage commitment. Immunity 2009; **30**(6):832-44.

Deng G, Podack ER. Suppression of apoptosis in a cytotoxic T-cell line by interleukin 2-mediated gene transcription and deregulated expression of the protooncogene bcl-2. Proc Natl Acad Sci USA 1993; **90**:2189-93.

Dong C, Nurieva RI. Regulation of immune and autoimmune responses by ICOS. J Autoimmun 2003; **21**:255-60.

Dooms H, Kahn E, Knoechel B, Abbas AK. IL-2 induces a competitive survival advantage in T lymphocytes. J Immunol 2004; **172**: 5973-79.

Dudda JC, Perdue N, Bachtanian E, Campbell DJ. Foxp3+ regulatory T cells maintain immune homeostasis in the skin. J Exp Med 2008; 205(7):1559-65.

Fontenot JD, Rasmussen JP, Gavin MA, Rudensky AY. A function for interleukin 2 in Foxp3-expressing regulatory T cells. Nat Immunol 2005; **6**:1142-51.

Forster R, Davalos-Misslitz AC, Rot A. CCR7 and its ligands: balancing immunity and tolerance. Nat Rev Immunol 2008; **8**(5):362-71.

Forster R, Schubel A, Breitfeld D, Kremmer E, Renner-Muller I, Wolf E, Lipp M. CCR7 coordinates the primary immune response by establishing functional microenvironments in secondary lymphoid organs. Cell 1999; **99**:23-33.

Freudenberg J et al. Genome-wide association study of rheumatoid arthritis in Koreans: population-specific loci as well as overlap with European susceptibility loci. Arthritis Rheum 2011; **63**:884-93.

Gasteiger G, Hemmers S, Firth MA, Le FA, Huse M, Sun JC, Rudensky AY. IL-2-independent tuning of NK cell sensitivity for target cells is controlled by regulatory T cells. J Exp Med 2013; **210**:1167-78.

Gavin MA, Rasmussen JP, Fontenot JD, Vasta V, Manganiello VC, Beavo JA, Rudensky AY. Foxp3-dependent programme of regulatory T-cell differentiation. Nature 2007; **445**:771-75.

Gigoux M, Shang J, Pak Y, Xu M, Choe J, Mak TW, Suh WK. Inducible costimulator promotes helper T-cell differentiation through phosphoinositide 3-kinase. Proc Natl Acad Sci USA 2009; **106**:20371-76.

Godfrey VL, Wilkinson JE, Russell LB. X-linked lymphoreticular disease in the scurfy (sf) mutant mouse. Am J Pathol 1991; **138**:1379-87.

Gratz IK, Truong HA, Yang SH, Maurano MM, Lee K, Abbas AK, Rosenblum MD. Cutting edge: Memory regulatory T cell require IL-7 and not IL-2 for their maintenance in peripheral tissues. J Immunol 2013; **190**.

Grundemann C et al. Cutting edge: Identification of E-cadherin as a ligand for the murine killer cell lectin-like receptor G1. J Immunol 2006; **176**:1311-1315.

Hall AO et al. The cytokines interleukin-27 and interferon-gamma promote distinct Treg cell populations required to limit infection-induced pathology. Immunity 2012; **37**:511-23.

Haxhinasto S, Mathis D, Benoist C. The AKT-mTOR axis regulates de novo differentiation of CD4+Foxp3+ cells. J Exp Med 2008; **205**(3):565-74.

Herman AE, Freeman GJ, Mathis D, Benoist C. CD4+CD25+ T regulatory cells dependent on ICOS promote regulation of effector cells in the prediabetic lesion. J Exp Med 2004; **199**(11):1479-89.

Hippen KL, Riley JL, June CH, Blazar BR. Clinical perspectives for regulatory T cells in transplantation tolerance. Semin Immunol 2011; **23**:462-68.

Hofmann M, Schweier O, Pircher H. Different inhibitory capacities of human and mouse KLRG1 are linked to distinct disulfide-mediated oligomerizations. Eur J Immunol 2012; **42**:2484-90.

Hori S, Nomura T, Sakaguchi S. Control of regulatory T cell development by the transcription factor Foxp3. Science 2003; **299**:1057-61.

Hoyer KK, Wolsiegel K, Dooms H, Abbas AK. Targeting T cell-specific costimulators and growth factors in a model of autoimmune hemolytic anemia. J Immunol 2007; **179**(5):2844-50.

Hsieh CS, Liang Y, Tyznik AJ, Self SG, Liggitt D, Rudensky AY. Recognition of the peripheral self by naturally arising CD25+CD4+ T cell receptors. Immunity 2004; **21**:267-277.

Huehn J, Siegmund K, Hamann A. Migration rules: functional properties of naïve and effector/memory-like regulatory T cell subsets. Curr Top Microbiol 2005; **293**:89-114.

Ito M, Maruyama T, Saito N, Koganei S, Yamamoto K, Matsumoto N. Killer cell lectin-like receptor G1 binds three members of the classical cadherin family to inhibit NK cell cytotoxicity. J Exp Med 2006; **203**:289-95.

Ito T et al. Two functional subsets of FOXP3+ regulatory T cells in human thymus and periphery. Immunity 2008; **28**:870-80.

Jenabian MA, Ancuta P, Gilmore N, Routy JP. Regulatory T cells in HIV infection: can immunotherapy regulate the regulator? Clin Dev Immunol 2012:908314.

Joshi NS et al. Inflammation directs memory precursor and short-lived effector CD8+ T cell fates via graded expression of T-bet transcription factor. Immunity 2007; **27**(2):281-95.

Kallies A et al. Transcriptional repressor Blimp-1 is essential for T cell homeostasis and self-tolerance. Nat Immunol 2006; **7**(5):466-74.

Killebrew JR, Perdue N, Kwan A, Thornton AM, Shevach EM, Campbell DJ. A self-reactive TCR drives the development of Foxp3+ regulatory T cells that prevent autoimmune disease. J Immunol 2011;**187**(2):861-9.

Kim HP, Kelly J, Leonard WJ. The basis for IL-2-induced IL-2 receptor alpha chain gene regulation: importance of two widely separated IL-2 response elements. Immunity 2001; **15**:159-72.

Kim JK, Klinger M, Benjamin J, Xiao Y, Erle DJ, Littman DR, Killeen N. Impact of the TCR signal on regulatory T cell homeostasis, function, and trafficking. PLoS One 2009; **4**(8):e6580.

Klonowski KD, Williams KJ, Marzo AL, Blair DA, Lingenheld EG, Lefrancois L. Dynamics of blood-borne CD8 memory T cell migration in vivo. Immunity 2004; **20**:551-62.

Koch MA, Tucker-Heard G, Perdue NR, Killebrew JR, Urdahl KB, Campbell DJ. T-bet controls regulatory T cell homeostasis and function during type-1 inflammation. Nat Immunol 2009; **10**(6):595-602.

Link A et al. Fibroblastic reticular cells in lymph nodes regulate the homeostasis of naïve T cells. Nat Immunol 2007; **8**(11):1255-65.

Linterman MA et al. Follicular helper T cells are required for systemic autoimmunity. J Exp Med 2009; **206**(3):561-76.

Liu G, Burns S, Huang G, Boyd K, Proia RL, Flavell RA, Chi H. The receptor S1P1 overrides regulatory T cell-mediated immune suppression through Akt-mTOR. Nat Immunol 2009; **10**(7):769-77.

Long SA, Buckner JH, Greenbaum CJ. IL-2 therapy in type 1 diabetes: 'trials' and tribulations. Clin Immunol 2013; **149**:324-31.

Luther SA, Tang HL, Hyman PL, Farr AG, Cyster JG. Coexpression of the chemokines ELC and SLC by T zone stromal cells and deletion of the ELC gene in the plt/plt mouse. Proc Natl Acad Sci USA 2000; **97**:12694-99.

Mahmud SA, Maniove LS, Farrar MA. Interleukin-2 and STAT5 in regulatory T cell development and function. JAKSTAT 2013; **2**(1):e23154.

Malchow S et al. Aire-dependent thymic development of tumor-associated regulatory T cells. Science 2013; **339**:1219-24.

Malek TR. The biology of interleukin-2. Annu Rev Immunol 2008; **26**:453-79.

Malek TR, Ashwell JD. Interleukin-2 upregulates expression of its receptor on a T cell clone. J Exp Med 1985; **161**:1575-1580.

Malek TR, Porter BO, Codias EK, Scibelli P, Yu A. Normal lymphoid homeostasis and lack of lethal autoimmunity in mice containing mature T cells with severely impaired IL-2 receptors. J Immunol 2000; **164**: 2905-14.

Malek TR, Yu A, Vincek V, Scibelli P, Kong L. CD4 regulatory T cells prevent lethal autoimmunity in IL-2Rbeta-deficient mice. Implications for the nonredundant function of IL-2. Immunity 2002; **17**:167-78.

Malhotra D, Fletcher AL, Turley SJ. Stromal and hematopoietic cells in secondary lymphoid organs: partners in immunity. Immunol Rev 2013; **251**:160-76.

Moran AE, Holzapfel KL, Xing Y, Cunningham NR, Maltzman JS, Punt J, Hogquist KA. T cell receptor signal strength in Treg and iNKT cell development demonstrated by a novel fluorescent reporter mouse. J Exp Med 2011; **208**:1279-89.

Ono M et al. Foxp3 controls regulatory T-cell function by interacting with AML1/Runx1. Nature 2007; **446**:685-89.

Ouyang W, Li MO. Foxo:in command of T lymphocyte homeostasis and tolerance. Trends Immunol 2011; **32**:26-33.

Ouyang W et al. Novel Foxo1-dependent transcriptional programs control T(reg) cell function. Nature 2012; **491**(7425):554-9.

Pandiyan P, Zheng L, Ishihara S, Reed J, Lenardo MJ. CD4+CD25+Foxp3+ regulatory T cells induce cytokine deprivation-mediated apoptosis of effector CD4+ T cells. Nat Immunol 2007; **8**:1353-62.

Patton DT et al. Cutting edge: the phosphoinositide 3-kinase p110 delta is critical for the function of CD4+CD25+Foxp3+ regulatory T cells. J Immunol 2006; **177**(10):6598-602.

Pierson W et al. Antiapoptotic Mcl-1 is critical for the survival and niche-filling capacity of Foxp3+ regulatory T cells. Nat Immunol 2013; **14**(9): 959-65.

Raychaudhuri S et al. Common variants at CD40 and other loci confer risk of rheumatoid arthritis. Nat Genet 2008; **40**:1216-23.

Read S, Malmstrom V, Powrie F. Cytotoxic T lymphocyte-associated antigen 4 plays an essential role in the function of CD25+CD4+ regulatory cells that control intestinal inflammation. J Exp Med 2000; **192**:295-302.

Rech AJ et al. CD25 blockade depletes and selectively reprograms regulatory T cells in concert with immunotherapy in cancer patients. Sci Transl Med 2012; **4**:134ra62.

Riley JL, June CH, Blazar BR. Human T regulatory cell therapy: take a billion or so and call me in the morning. Immunity 2009; **30**:656-65.

Robbins SJ, Hguyen KB, Takahashi N, Mikayama T, Biron CA, Brossay L. Cutting edge: inhibitory functions of the killer cell lectin-like receptor G1 molecule during the activation of mouse NK cells. J Immunol 2002; **168**:2585-89.

Robbins SH, Terrizzi SC, Sydora BC, Mikayama T, Brossay L. Differential regulation of killer cell lectin-like receptor G1 expression on T cells. J Immunol 2003; **170**:5876-85.

Rosenblum MD, Gratz IK, Paw JS, Lee K, Marshak-Rothstein A, Abbas AK. Response to self antigen imprints regulatory memory in tissues. Nature 2011; **480**:538-42.

Rubtsov YP et al. Regulatory T cell-derived interleukin-10 limits inflammation at environmental surfaces. Immunity 2008; **28**(4):546-58.

Sabatos CA, Doh J, Chakravarti S, Friedman RS, Pandurangi PG, Tooley AJ, Krummel MF. A synaptic basis for paracrine interleukin-2 signaling during homotypic T cell interaction. Immunity 2008; **29**(2):238-48.

Sage PT, Francisco LM, Carman CV, Sharpe AH. The receptor PD-1 controls follicular regulatory T cells in the lymph nodes and blood. Nat Immunol 2013; **14**(2):152-61.

Sakaguchi S, Yamaguchi T, Nomura T, Ono M. Regulatory T cells and immune tolerance. Cell 2008; **133**:775-87.

Salomon B. Lenschow DJ, Rhee L, Ashourian N, Singh B, Sharpe A, Bluestone JA. B7/CD28 costimulation is essential for the homeostasis of the CD4+CD25+ immunoregulatory T cells that control autoimmune diabetes. Immunity 2000; **12**(4);431-40.

Sallusto F, Lenig D, Forster R, Lipp M, Lanzavecchia A. Two subsets of memory T lymphocytes with distinct homing potential and effector functions. Nature 1999; **401**:708-12.

Sallusto F, Mackay CR. Chemoattractants and their receptors in homeostasis and inflammation. Curr Opin Immunol 2004; **16**:724-31.

Sather BD, Treuting P, Perdue N, Miazgowicz M, Fontenot JD, Rudensky AY, Campbell DJ. Altering the distribution of Foxp3(+) regulatory T cells results in tissue-specific inflammatory disease. J Exp Med 2007; **204**(6):1335-47.

Schneider MA, Meingassner JG, Lipp M, Moore HD, Rot A. CCR7 is required for the in vivo function of CD4+CD25+ regulatory T cells. J Exp Med 2007; **204**:735-45.

Setoguchi R, Hori S, Takahashi T, Sakaguchi S. Homeostatic maintenance of nature Foxp3+CD25+CD4+ regulatory T cells by interleukin (IL)-2 and induction of autoimmune disease by IL-2 neutralization. J Exp Med 2005; **201**(5):723-35.

Simpson TR, Quezada SA, Allison JP. Regulation of CD4 T cell activation and effector function by inducible costimulatory (ICOS). Curr Opin Immunol 2010; **22**:326-32.

Sitrin J, Ring A, Garcia KC, Benoist C, Mathis D. Regulatory T cells control NK cells in an insulitic lesion by depriving them of IL-2. J Exp Med 2013; **210**:1153-65.

Soper DM, Kasprowicz DJ, Ziegler SF. IL-2Rbeta links IL-2R signaling with Foxp3 expression. Eur J Immunol 2007; **37**:1817-26.

Tadokoro CE et al. Regulatory T cells inhibit stable contacts between CD4+ T cells and dendritic cells in vivo. J Exp Med 2006; **203**: 505-11.

Tai X et al. Foxp3 transcription factor is proapoptotic and lethal to developing regulatory T cells unless counterbalanced by cytokine survival signals. Immunity 2013; **38**(6): 1116-28.

Tang Q, Bluestone JA, Kang SM. CD4+Foxp3+ regulatory T cell therapy in transplantation. J Mol Cell Biol 2012; **4**:11-21.

Tang Q et al. Central role of defective IL-2 production in the triggering of islet autoimmune destruction. Immunity 2008; **28**:687-97.

Thorton AM, Korty PE, Tran DQ, Wohlfert EA, Murray PE, Belkaid Y, Shevach EM. Expression of Helios, an Ikaros transcription factor family member, differentiates thymic-derived from peripherally induced Foxp3+ T regulatory cells. J Immunol 2010; **184**:3433-3441.

Takahashi T, Kuniyasu T, Toda M, Sakaguchi N, Itoh M, Iwata M, Shimizu J, Sakaguchi S. Immunologic self-tolerance maintained by CD25+CD4+ naturally anergic and suppressive T cells: induction of autoimmune disease by breaking their anergic/suppressive state. Int Immuno 1998; **10**:1969-80.

Tan AH, Wong SC, Lam KP. Regulation of mouse inducible costimulator (ICOS) expression by Fyn-NFATc2 and ERK signaling in T cells. J Biol Chem 2006; **281**:28666-78.

Tang Q et al. Cutting edge: CD28 controls peripheral homeostasis of CD4+CD25+ regulatory T cells. J Immunol 2003; **171**(7):3348-52.

Tang Q et al. Central role of defective interleukin-2 production in the triggering of islet autoimmune destruction. Immunity 2008; **28**:687-97.

Vang KB, Yang J, Mahmud SA, Burchill MA, Vegoe AL, Farrar MA. IL-2, -7, and -15, but not thymic stromal lymphopoeitin, redundantly govern CD4+Foxp3+ regulatory T cell development. J Immunol 2008; **181**(5):3285-90.

Vignali DA, Collison LW, Workman CJ. How regulatory T cells work. Nat Rev Immunol 2008; **9**:632-640.

Von Boehmer H. Mechanisms of suppression by suppressor T cells. Nat Immunol 2005; **6**:338-344.

Walker LS, Chodos A, Eggena M, Dooms H, Abbas AK. Antigen-dependent proliferation of CD4+CD25+ regulatory T cells in vivo. J Exp Med 2003; **198**:249-58.

Wang J, Wicker LS, Santamaria P. IL-2 and its high-affinity receptor: genetic control of immunoregulation and autoimmunity. Semin Immunol 2009; **21**:363-71.

Webster KE et al. In vivo expansion of Treg cells with IL-2-mAb complexes: induction of resistance to EAE and long-term acceptance of islet allografts without immunosuppression. J Exp Med 2009; **206**(4):751-60.

Willerford DM, Chen J, Ferry JA, Davidson L, Ma A, Alt FW. Interleukin-2 receptor alpha chain regulates the size and content of the peripheral lymphoid compartment. Immunity 1995; **3**:521-30.

Williams MA, Tyznik AJ, Bevan MJ. Interleukin-2 signals during priming are required for secondary expansion of CD8+ memory T cells. Nature 2006; **441**: 890-93.

Wojciechowski S et al. Bim/Bcl-2 balance is critical for maintaining naïve and memory T cell homeostasis. J Exp Med 2007; **204**(7):1655-75.

Worbs T, Mempel TR, Bolter J, von Adrian UH, Forster R. CCR7 ligands stimulate the intranodal motility of T lymphocytes in vivo. J Exp Med 2007; **204**(3):489-95.

Yadav M et al. Neuropilin-1 distinguishes natural and inducible regulatory T cells among regulatory T cell subsets in vivo. J Exp Med 2012; **209**:1713-19.

Yadav M, Stephan S, Bluestone JA. Peripherally induced Tregs- role in immune homeostasis and autoimmunity. Front Immunol; **4**:232.

Zeng H, Yang K, Cloer C, Neale G, Vogel P, Chi H. mTORC1 couples immune signals and metabolic programming to establish T(reg)-cell function. Nature 2013; **499**(7459):485-90.

Zhang R, Huynh A, Whitcher G, Chang J, Maltzman JS, Turka LA. An obligate cell-intrinsic function for CD28 in Tregs. J Clin Ivest 2013; **123**(2):580-93.

Zheng Y et al. Regulatory T-cell suppressor program co-opts transcription factor IRF4 to control Th2 responses. Nature 2009; **458**(7236):351-6.